CHEMISTRY OF MATERIALS
Article

Chem. Mater. **2010,** *22,* 2869–2884 2869
DOI:10.1021/cm100134f

Achiral Bent-Core Molecules with a Series of Linear or Branched Carbosilane Termini: Dark Conglomerate Phases, Supramolecular Chirality and Macroscopic Polar Order

Yongqiang Zhang,*,† Ute Baumeister,‡ Carsten Tschierske,*,§ Michael J. O'Callaghan,† and Christopher Walker†

†*Displaytech, Inc. (now part of Micron Technology, Inc.), 2601 Clover Basin Drive, Longmont, Colorado 80503,* ‡*Department of Physical Chemistry, Institute of Chemistry, Martin Luther University Halle–Wittenberg, Kurt-Mothes-Strasse 2, 06120 Halle, Germany, and* §*Department of Organic Chemistry, Institute of Chemistry, Martin Luther University Halle–Wittenberg, Kurt-Mothes-Strasse 2, 06120 Halle, Germany*

Received January 15, 2010. Revised Manuscript Received March 1, 2010

New organic–inorganic hybrid materials that combine a bent π-conjugated aromatic core with one linear or branched carbosilane unit have been synthesized and investigated, with respect to their self-assembly in liquid crystalline (LC) phases, by means of polarizing microscopy, differential scanning calorimetry (DSC), X-ray diffraction (XRD), and electro-optical techniques. Most of these achiral compounds show spontaneous symmetry breaking into chiral superstructures that represent conglomerates with macroscopic domains of opposite handedness. These fluid chiral superstructures can be frozen into the glassy state and, for one of the compounds, chirality was switched under the application of a special waveform of an applied external electric field between two enantiomeric states. This flipping of supramolecular chirality occurs between oppositely tilted structures, which represents a new mode of chirality switching. Besides spontaneous chirality, these materials show polar order, leading to ferroelectric (FE) and antiferroelectric (AF) switching modes. For one compound with a highly branched carbosilane unit, a temperature-, voltage-, and frequency-dependent reversible transition from AF switching with inversion of chirality to FE switching with retention of chirality was observed. Models were developed to explain the experimental observations, based on enthalpic and entropic contributions of distinct supermolecular arrangements in these soft matter systems.

Introduction

Macroscopic polar order is an important materials property, for example, leading to piezoelectricity, pyroelectricity, and nonlinear optical activity.[1] Chirality and spontaneous separation of mirror images in supermolecular structures play a key role in stereochemistry and provide great opportunities across a spectrum of disciplines: from medicinal chemistry to materials science.[2,3] Both concepts were first developed in crystalline systems, later on extended to thin films but, until recently, seemed unlikely to occur in fluids. Recent discoveries that nonchiral bent-core (bow or banana-shaped) molecules[4,5] can organize into fluid, liquid crystalline (LC) phases with polar order and macroscopic chirality[6,7] opened an intriguing area of materials research, as noted in recent highlights.[8,9]

The polar order in these mesophases results from the restricted rotation of the closely packing bent-core molecules around their long axes, while the chirality arises from the tilted organization of these molecules in polar layers. Opposite handedness, (+) and (−), is described by a right- or left-handed system determined by layer-normal, tilt-direction, and bend-direction (see Figure 1). Thus, the handedness, (+) and (−), is determined by the relationship among three vectors, $\hat{b} = \hat{z} \times \hat{n}$, in a right- or left-handed system described by layer-normal ($\hat{z}$), tilt-direction ($\hat{n}$), and bend-direction ($\hat{b}$) (see Figures 1a and 1b). Changing either the bend direction or the tilt direction reverses the handedness of layers, while changing both retains the handedness (see Figure 1c).[10]

---

*Author to whom correspondence should be addressed. E-mail addresses: yqzhang@micron.com; tschierske@chemie.uni-halle.de.

(1) Sayar, M.; Olvera de la Cruz, M.; Stupp, S. I. *Europhys. Lett.* **2003**, *61*, 334–340.
(2) *Chirality–From Weak Bosons to the α-Helix*; Janoschek, R., Ed.; Springer: Berlin, 1991.
(3) Pérez-García, L.; Amabilino, D. B. *Chem. Soc. Rev.* **2002**, *31*, 342–356.
(4) Niori, T.; Sekine, T.; Watanabe, J.; Furukawa, T.; Takezoe, H. *J. Mater. Chem.* **1996**, *6*, 1231–1233.
(5) Reviews: (a) Reddy, R. A.; Tschierske, C. *J. Mater. Chem.* **2006**, *16*, 907–961. (b) Takezoe, H.; Takanishi, Y. *Jpn. J. Appl. Phys.* **2006**, *45*, 597–625. (c) Etxebarria, J.; Ros, M. B. *J. Mater. Chem.* **2008**, *18*, 2919–2916.
(6) Link, D. R.; Natale, G.; Shao, R.; Maclennan, J. E.; Clark, N. A.; Körblova, E.; Walba, D. M. *Science* **1997**, *278*, 1924.
(7) Hough, L. E.; Spannuth, M.; Nakata, M.; Coleman, D. A.; Jones, C. D.; Dantlgraber, G.; Tschierske, C.; Watanabe, J.; Körblova, E.; Walba, D. M.; Maclennan, J. E.; Glaser, M. A.; Clark, N. A. *Science* **2009**, *325*, 452–456.
(8) Amabilino, D. B. *Science* **2009**, *325*, 402–403.
(9) Dierking, I. *Angew. Chem., Int. Ed.* **2010**, *49*, 29–30.

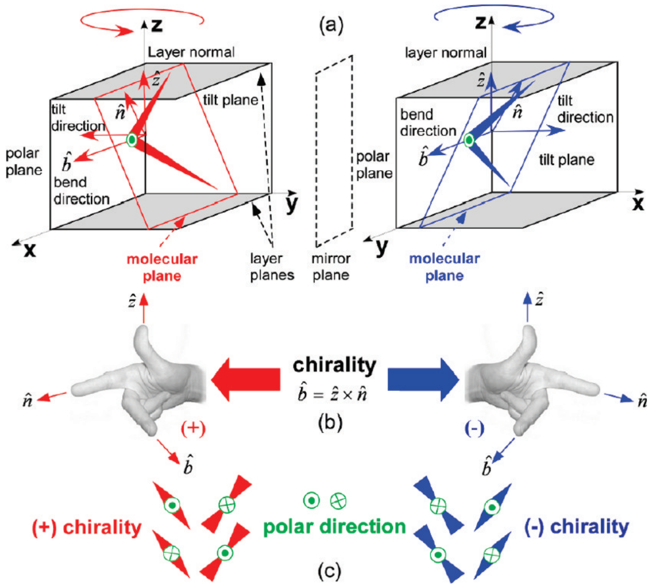

Figure 1. Organization of bent-core molecules in polar SmCP phases, indicating the origin of superstructural chirality. (a) Right-handed (left) and left-handed (right) Cartesian coordinate systems are defined by the relationship among three vectors. The geometries of molecules with opposite chirality were drawn in different colors (red = (+) chirality, blue = (−) chirality). The drawing shows one possible direction of the polar vector, parallel to the bend direction. (b) The chirality (+) or (−) of molecules can be determined by the right- or left-hand rule. (c) All four possible arrangements for bent-core molecules with macroscopic (+) (red) and (−) (blue) chirality are shown with opposite polarity (green). Note that the correct choice of a set of drawings in panel c is necessary for an accurate description of molecular orientations under a field.

In bent-core smectic (B2) phases, the four basic structures, SmC$_s$P$_A$ (racemic), SmC$_a$P$_A$ (chiral), SmC$_s$P$_F$ (chiral), and SmC$_a$P$_F$ (racemic) are possible, because the tilt and bend directions (= polar direction) in adjacent layers could be either identical or opposite (see Figure S1 in the Supporting Information). Herein, the lowercase subscripts ("s" and "a") denote syn- and anticlinicity of tilt, while the capital subscripts ("F" and "A"), denote ferroelectricity and antiferroelectricity (P$_F$ = FE, P$_A$ = AF), respectively.[11] Most bent-core molecules possess antiferroelectric layer structures (SmCP$_A$) that can be switched to the corresponding FE states upon the application of a sufficiently strong external electric field. This AF switching process is characterized by two polarization current peaks in each half period of the applied triangular wave (TW) voltage and is also called tristable switching, as the polar FE states relax to a nonpolar AF state at 0 V. A few bent-core molecules have been reported to exhibit FE switching mesophases.[12] This bistable process switches directly between the two polar FE states without relaxation to an apolar AF state and, hence, it is characterized by only one polarization current peak in each half period of the applied TW voltage.

Two different switching mechanisms—rotation of the molecules (i) on the tilt cone or (ii) around their long axes—were observed for a variety of bent-core molecules (see Figure S3 in the Supporting Information). The first switching mechanism changes only the polarity of layers while retaining their chirality, and the second changes both the polarity and chirality.

Some bent-core molecules can organize into ground-state dark conglomerate (DC) mesophases,[13,14] in which macroscopic chirality can be identified under a polarizing microscope by slightly uncrossing the polarizer and the analyzer. Under this condition, domains that consist of dark and bright regions can be identified. Reversing the directions of the polarizer and analyzer reverses the brightness of these domains. This indicates that these mesophases are composed of a conglomerate of macroscopic domains of opposite handedness. The optical activity is attributed to the inherent chirality of the polar SmCP layers, but it can be observed only if the mesophase structure is homogeneously chiral, i.e., for a SmC$_a$P$_A$ or SmC$_s$P$_F$ structure.[15] The molecular organization of the DC phase has recently been established by using freeze fracture transmission electron microscopy (TEM) and X-ray diffraction (XRD).[7] TEM images show the local smectic layering and saddle splay layer deformation in the DC phase. The molecular organization resembles in topography that of the lyotropic sponge phase.[16] Because

---

(10) Depending on the molecular structure the polar direction could be either parallel or antiparallel to the bend-direction, while the bend direction is exclusive and coincides with the polar C_2-axis. To avoid causing confusion, we herein propose to use the bend direction instead of the polar direction to define absolute supramolecular chirality.

(11) Keith, C.; Reddy, R. A.; Hauser, A.; Baumeister, U.; Tschierske, C. *J. Am. Chem. Soc.* **2006**, *16*, 3051–3066.

(12) Examples of nonsilylated FE switching bent-core materials: (a) Walba, D. M.; Körblova, E.; Shao, R.; Maclennan, J. E.; Link, D. R.; Glaser, M. A.; Clark, N. A. *Science* **2000**, *288*, 2181–2184. (b) Nakata, M.; Link, D. R.; Araoka, F.; Thisayukta, J.; Takanishi, Y.; Ishikawa, K.; Watanabe, J.; Takezoe, H. *Liq. Cryst.* **2001**, *28*, 1301–1308. (c) Bedel, J. P.; Rouillon, J. C.; Marcerou, J. P.; Laguerre, M.; Nguyen, H. T.; Achard, M. F. *J. Mater. Chem.* **2002**, *12*, 2214–2220. (d) Reddy, R. A.; Sadashiva, B. K. *J. Mater. Chem.* **2002**, *12*, 2627–2642. (e) Reddy, R. A.; Sadashiva, B. K. *Liq. Cryst.* **2003**, *30*, 1031–1050. (f) Rauch, S.; Bault, P.; Sawade, H.; Heppke, G.; Nair, G. G.; Jakli, A. *Phys. Rev. E* **2002**, *66*, 021706. (g) Kumazawa, K.; Nakata, M.; Araoka, F.; Takanishi, Y.; Ishikawa, K.; Watanabe, J.; Takezoe, H. *J. Mater. Chem.* **2004**, *14*, 157–164. (h) Reddy, R. A.; Raghunathan, V. A.; Sadashiva, B. K. *Chem. Mater.* **2005**, *17*, 274–283. (i) Nadasi, H.; Weissflog, W.; Eremin, A.; Pelzl, G.; Diele, S.; Das, S.; Grande, S. *J. Mater. Chem.* **2002**, *12*, 1316–1324. (j) Bedel, J. P.; Rouillon, J. C.; Marcerou, J. P.; Nguyen, H. T.; Achard, M. F. *Phys. Rev. E* **2004**, *69*, 061702. (k) Lee, S. K.; Heo, S.; Lee, J.-G.; Kang, K.-T.; Kumazawa, K.; Nishida, K.; Shimbo, Y.; Takanishi, Y.; Watanabe, J.; Doi, T.; Takahashi, T.; Takezoe, H. *J. Am. Chem. Soc.* **2005**, *127*, 11085–11091. (l) Nishida, K.; Cepic, M.; Kim, W. J.; Lee, S. K.; Heo, S.; Lee, J. G.; Takanishi, Y.; Ishikawa, K.; Kang, K.-T.; Watanabe, J.; Takezoe, H. *Phys. Rev. E.* **2006**, *74*, 021704. (m) Reddy, R. A.; Schröder, M. W.; Bodyagin, M.; Kresse, H.; Diele, S.; Pelzl, G.; Weissflog, W. *Angew. Chem.* **2005**, *117*, 784–788. *Angew. Chem., Int. Ed.* **2005**, *44*, 774−778.

(13) Dark conglomerate phases of nonsilylated molecules: (a) Thisayukta, J.; Nakayama, Y.; Kawauchi, S.; Takezoe, H.; Watanabe, J. *J. Am. Chem. Soc.* **2000**, *122*, 7441–7448. (b) Thisayukta, J.; Kamee, H.; Kawauchi, S.; Watanabe, J. *Mol. Cryst. Liq. Cryst.* **2000**, *346*, 63–75. (c) Shreenivasa Murthy, H. N.; Sadashiva, B. K. *Liq. Cryst.* **2002**, *29*, 1223–1234. (d) Ortega, J.; Folcia, C. L.; Etxebarria, J.; Gimeno, N.; Ros, M. B. *Phys. Rev. E* **2003**, *68*, 011707. (e) Weissflog, W.; Schröder, M. W.; Diele, S.; Pelzl, G. *Adv. Mater.* **2003**, *15*, 630–633. (f) Jakli, A.; Huang, Y.-M.; Fodor-Csorba, K.; Vajda, A.; Galli, G.; Diele, S.; Pelzl, G. *Adv. Mater.* **2003**, *15*, 1606–1610. (g) Schröder, M. W.; Diele, S.; Pelzl, G.; Dunemann, U.; Kresse, H.; Weissflog, W. *J. Mater. Chem.* **2003**, *13*, 1877–1882. (h) Schröder, M. W.; Pelzl, G.; Dunemann, U.; Weissflog, W. *Liq. Cryst.* **2004**, *31*, 633–637. (i) Weissflog, W.; Sokolowski, S.; Dehne, H.; Das, B.; Grande, S.; Schröder, M. W.; Eremin, A.; Diele, S.; Pelzl, G.; Kresse, H. *Liq. Cryst.* **2004**, *31*, 923–933.

(14) Field-induced SmCP$^{[*]}$ phases: (a) Heppke, G.; Parghi, D. D.; Sawade, H. *Liq. Cryst.* **2000**, *27*, 313–320. (b) Etxebarria, J.; Folcia, C. L.; Ortega, J.; Ros, M. B. *Phys. Rev. E* **2003**, *67*, 042702.

(15) Hough, L. E.; Clark, N. A. *Phys. Rev. Lett.* **2005**, *95*, 107802.

of this local disorder, these mesophases appear optically isotropic (dark).

Incorporation of terminal siloxane units at one or two tails of bent-core molecules yields DC phases, which behave as ferroelectric (FE) switching smectic phases upon the application of a sufficiently strong external electric field.[17] This class of bent-core molecules consists of three incompatible units: one rigid aromatic core, two floppy alkyl chains, and one or two bulky siloxane termini. In these compounds, oligosiloxane units form sublayers, leading to microsegregation between aliphatic chains and oligosiloxane units. This segregation reduces interlayer fluctuations, which diminishes the entropic preference of the AF structure (see Figure S2 in the Supporting Information), thereby enabling the formation of FE layer structures ($SmCP_F$),[11] which adopt a sponge-like deformation in the ground state (as shown in Figure 5c, presented later in this work).[7]

As far as practical applications are concerned, carbosilanes are significantly advantageous over siloxanes, because of their greater chemical stability.[18] For instance, siloxane units are sensitive to moisture and can degrade under even weakly acidic conditions, while carbosilane units are completely stable under these conditions. Moreover, a richer variety of carbosilanes can be synthesized, allowing the design of longer and more branched silyl groups.[19] The previously reported carbosilane-substituted bent-core molecules (monomers,[18] dimers,[20] and dendrimers[21]) possess two or three methylene (CH$_2$) units between Si atoms. Hence, the dimethylsilyl units in the carbosilane mesogens are more apart than in their siloxane analogues and, therefore, cannot be directly compared with the corresponding siloxanes.

Chart 1. Bent-Core Compounds (**Si$_x$B*m***) under Investigation[a]

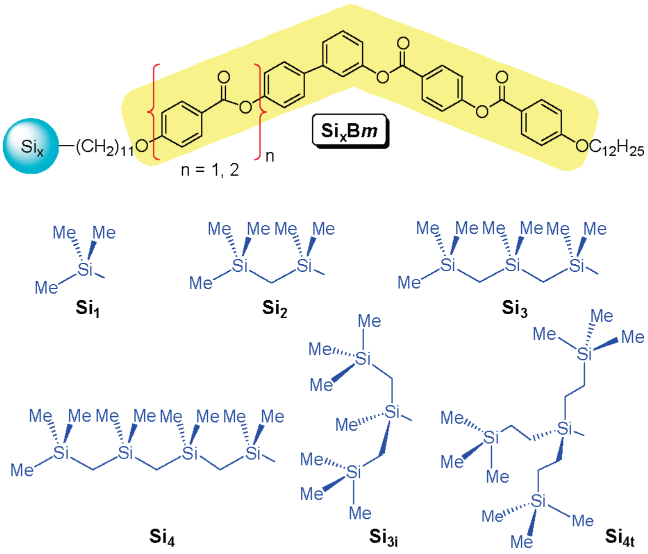

[a] B represents the bent aromatic core (yellow highlighted area); m is the number of phenyl rings ($m = n + 4$); Si$_x$ denotes the linear and branched carbosilyl units (shown in blue) that are illustrated as Si$_1$, Si$_2$, Si$_3$, Si$_4$, Si$_{3i}$, and Si$_{4t}$ at the bottom; and x is the number of Si atoms in the carbosilane units.

Herein, we first report bent-core molecules (**Si$_x$B*m***) that incorporate a series of linear or branched carbosilane termini (see Chart 1) that have only one methylene unit between adjacent Si atoms (Si$-$CH$_2-$Si), which are isosteric to their siloxane (Si$-$O$-$Si) counterparts but much more stable. Only for the most branched compounds **Si$_{4t}$B5**[19] and **Si$_{4t}$B6**, were ethylene groups used instead of the methylene groups to connect the silyl groups. Two series of compounds were investigated: compounds **Si$_x$B5** with a relatively short aromatic core consist of only five aromatic rings, and the longer compounds **Si$_x$B6** have six aromatic rings. In both series, optically isotropic smectic mesophases composed of a conglomerate of macroscopic domains with opposite chirality (DC phases) form in the absence of an electric field and birefringent smectic phases with a synclinic tilted polar SmC_sP_F structure develop under a low-frequency electric field. Compounds **Si$_x$B6** with a longer aromatic core represent the first FE switching bent-core mesogens whose DC phases are supercooled to the glassy state. In the **Si$_x$B5** series, as the carbosilane units change from linear to a highly branched one (Si$_{4t}$), a transition from smectic DC phases to a columnar phase ($Col_{ob}P_A$) is found in **Si$_{4t}$B5**. Moreover, in the smectic phases under high-frequency AC fields, a structural transition was observed from the synclinic SmC_sP_F structure to an anticlinic $[SmC_sP_F]_aP_S$ structure composed of SmC_sP_F layer stacks with anticlinic and synpolar interfaces (SmC_aP_F defect layers).[22,23] In the smectic compounds **Si$_x$B*m***, this transition is *irreversible*, whereas

---

(16) (a) DiDonna, B. A.; Kamien, R. D. *Phys. Rev. Lett.* **2002**, *89*, 215504. (b) Strey, R.; Winkler, J.; Magid, L. *J. Phys. Chem.* **1991**, *95*, 7502–7507.

(17) Dantlgraber, G.; Eremin, A.; Diele, S.; Hauser, A.; Kresse, H.; Pelzl, G.; Tschierske, C. *Angew. Chem.* **2002**, *114*, 2514–2518. *Angew. Chem., Int. Ed.* **2002**, *41*, 2408–2412.

(18) Keith, C.; Reddy, R. A.; Hahn, H.; Lang, H.; Tschierske, C. *Chem. Commun.* **2004**, 1898–1899.

(19) Preliminary report of compound **Si$_{4t}$B5**: Zhang, Y.; O'Callaghan, M. J.; Baumeister, U.; Tschierske, C. *Angew. Chem.* **2008**, *120*, 6998–7002. *Angew. Chem., Int. Ed.* **2008**, *47*, 6892–6896.

(20) Keith, C.; Reddy, R. A.; Baumeister, U.; Hahn, H.; Lang, H.; Tschierske, C. *J. Mater. Chem.* **2006**, *16*, 3444–3447.

(21) (a) Dantlgraber, G.; Baumeister, U.; Diele, S.; Kresse, H.; Lühmann, B.; Lang, H.; Tschierske, C. *J. Am. Chem. Soc.* **2002**, *124*, 14852–14853. (b) Hahn, H.; Keith, C.; Lang, H.; Reddy, R. A.; Tschierske, C. *Adv. Mater.* **2006**, *18*, 2629–2633.

(22) Keith, C.; Reddy, R. A.; Prehm, M.; Baumeister, U.; Kresse, C. H.; Chao, J. L.; Hahn, H.; Lang, H.; Tschierske, C. *Chem.—Eur. J.* **2007**, *13*, 2556.

(23) This layer stacking model is supported by the fact that a SmC_sP_A material exhibits a striped circular domain with anticlinic brushes despite the synclinic organization in a number of layers (see ref 23a). $[SmC_sP_F]_aP_S$ is optically identical to the classic SmC_aP_F structure with anticlinicity between adjacent polar layers if the length of SmC_sP_F stacks is shorter than the wavelength of light. In a circular domain, extinction brushes, in both cases, coincide with the directions of the polarizer and analyzer. The difference between these two structural models is the number of anticlinic interfaces. If anticlinic interfaces are equal to half the number of layers, the two models are identical, and if the number of interfaces is so small that the length of SmC_sP_F stacks is longer than the wavelength of light, a striped circular domain with anticlinic defects should be observed. It was reported that the classic model of the SmC_aP_F structure induced from the SmC_sP_A structure via rotation of molecules on a cone upon the application of an electric field would be in conflict with the Curie principle. The stacked layer model does not have this problem. See discussion in ref 23b on the classic SmC_aP_F structure being in conflict with the Curie principle. (a) Zennyoji, M.; Takanishi, Y.; Ishikawa, K.; Thisayukta, J.; Watanabe, J.; Takezoe, H. *J. Mater. Chem.* **1999**, *9*, 2775–2778. (b) Folcia, C. L.; Ortega, J.; Etxebarria, J. *Liq. Cryst.* **2003**, *30*, 1189–1191.

Scheme 1. Synthesis of 4-Alkoxybenzoic Acids Incorporating Terminal Carbosilane Units[a]

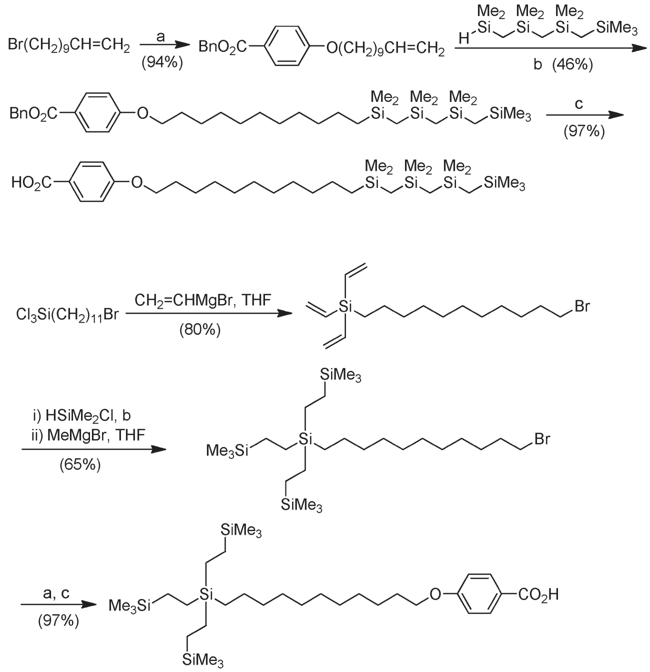

[a] (a) 4-benzyloxybenzoic acid, DCC, DMAP, CHCl$_3$, room temperature, overnight; (b) Karstedt's catalyst, toluene, room temperature, overnight; (c) Pd(OH)$_2$/C, H$_2$, EtOAc, room temperature, overnight.

Scheme 2. Synthesis of Bent-Core Compounds[a]

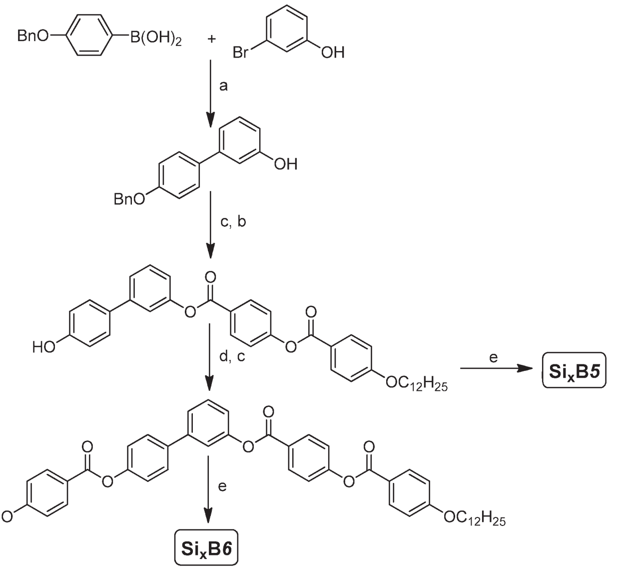

[a] (a) Pd(PPh$_3$)$_4$, 2 M Na$_2$CO$_3$ aqueous solution, DME, reflux, 15 h;[25] (b) 4-(4-*n*-dodecyloxybenzoyloxy)benzoic acid,[26] DCC, DMAP, CHCl$_3$, room temperature, overnight; (c) Pd(OH)$_2$/C, H$_2$, EtOAc, room temperature, overnight; (d) 4-benzyloxybenzoic acid, DCC, DMAP, CHCl$_3$, room temperature, overnight; (e) 4-(11-silylundecyloxy)benzoic acid (see synthesis details in the Supporting Information), DCC, DMAP, CHCl$_3$, room temperature, overnight.[27]

it is *reversible* for **Si$_{4t}$B*5*** with a columnar ground-state structure. For **Si$_{4t}$B*5***, we observed an unexpected temperature-, frequency-, and voltage-dependent reversible transition from antiferroelectric (AF) switching via rotation of the molecules around the molecular long axis to FE switching[24] via rotation of the molecules on a cone. Based on this voltage- and frequency-dependent reorganization of these molecules, we designed a waveform that yields field-induced supramolecular chirality flipping between oppositely tilted structures with identical polar direction,[19]which is an unprecedented mode of switching supramolecular chirality in bent-core LC superstructures.

Results and Discussion

1. Synthesis. The synthesis of two representative 4-alkoxybenzoic acids incorporating a terminal linear (Si$_4$) or a branched (Si$_{4t}$) carbosilane unit in two different approaches is shown in Scheme 1. Other 4-alkoxybenzoic acids with terminal carbosilyl groups (Si$_1$, Si$_2$, Si$_3$, and Si$_{3i}$) were similarly synthesized (see synthesis details in the Supporting Information). The synthesis of compounds **Si$_x$B*5*** and **Si$_x$B*6*** is shown in Scheme 2 (see detailed synthesis procedures and analytic data in the Supporting Information).[25,26] In contrast to the synthesis of the previously reported siloxanes and carbosilanes where the silyl groups had to be introduced via hydrosilylation reaction in the very last synthetic step, for the synthesis of compounds **Si$_x$B*5*** and **Si$_x$B*6***, benzoic acids with carbosilyl substituents were esterified[27] with bent-core phenols to afford the final carbosilane mesogens **Si$_x$B*m***. This approach enables a richer variety of carbosilane mesogens. Purification was done via flash chromatography (twice) and crystallization from a mixture of hexane and ethyl acetate. Analytical data are in good agreement with the proposed structures. The liquid crystalline phases were characterized by polarized-light optical microscopy (POM), differential scanning calorimetry (DSC),[28] X-ray diffraction (XRD), and electro-optical techniques.

---

(24) Herein ferroelectric (FE) switching is used to denote a polar single peak switching between the two field-induced polar states with opposite signs, where switching current curves show only one single peak upon the application of a triangular wave (TW) voltage and optical investigations confirm bistable switching. Proper FE switching is always related to the ferroelectricity of the ground-state structure. If the ferroelectric states are only metastable (due to surface stabilization or if there is not sufficient time (at 0 V) to allow the polar states to relax to the ground-state AF structure), the switching process is more precisely assigned as polar single peak switching. Thus ground-state AF materials always exhibit polar single peak switching upon the application of a square wave (SW) voltage. As we observed single-peak switching and optical bistability under TW fields also at very low frequencies, we use the more common term "FE switching", although we cannot fully exclude that the ferroelectric states might be field-induced or surface-stabilized long-lived metastable states.

(25) (a) Miyaura, N.; Suzuki, A. *Chem. Rev.* **1995**, *95*, 2457–2483. (b) Hird, M.; Gray, G. W.; Toyne, K. J. *Mol. Cryst. Liq. Cryst.* **1991**, *206*, 187–204.

(26) Shen, D.; Pegenau, A.; Diele, S.; Wirth, I.; Tschierske, C. *J. Am. Chem. Soc.* **2000**, *122*, 1593–1601.

(27) Tschierske, C.; Zaschke, H. *J. Prakt. Chem.* **1989**, *331*, 365–366.

(28) Melting points strongly depend on the history of the sample. To keep the consistency of phase transition temperatures, samples for DSC measurements were initially heated to the isotropic liquid and then stored in vials at room temperature for 3 days prior to DSC measurements, except as noted.

(29) In the phase assignment SmCP$_{FE}$$^{[*]}$, the C stands for a tilted organization of the molecules in the layers, P indicates polar order in the layers, the subscript "FE" denotes that ferroelectric switching is observed experimentally, and the superscripted symbol "[*]" denotes that, in the ground-state structure, a texture composed of a conglomerate of chiral domains with opposite handedness (see Figures 2a and 2b) can be observed (although the molecules themselves are achiral).

Table 1. Mesophases, Phase-Transition Temperatures and Enthalpies, Lattice Parameters, Outer Diffuse Scatterings (ODSs), and Spontaneous Polarizations of Compounds[a]

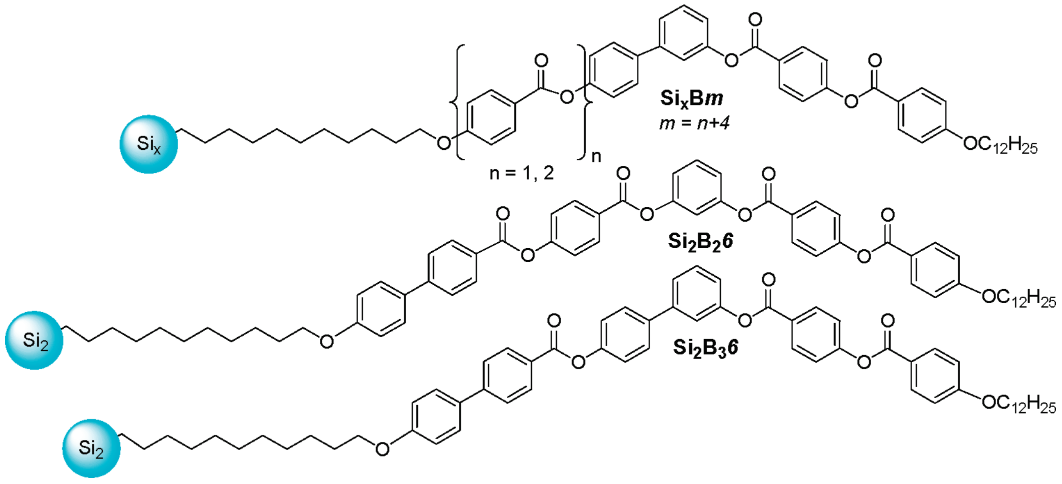

compound	mesophase and phase-transition temperature[b]		parameters d, a, b, and γ[c]	ODS, d (nm)[c]	P_s (nC/cm^2)[c]
Si$_1$B5	Cr 115 $\mathrm{SmCP_{FE}}^{[*/\circ]}$ *33.6*	118 Iso *25.1*	d = 3.84 nm (100)	nd	850 (105)
Si$_2$B5	Cr 84 $\mathrm{SmCP_{FE}}^{[*]}$ *23.9*	114 Iso *26.2*	d = 4.10 nm (100)	nd	810 (100)
Si$_3$B5	Cr 72 $\mathrm{SmCP_{FE}}^{[*]}$ *15.7*	112 Iso *26.9*	d = 4.46 nm (100)	0.47, 0.56 (100)	750 (100)
Si$_{3i}$B5[d]	Cr$_1$ 67 Cr$_2$ 74 $\mathrm{SmCP_{FE}}^{[*]}$ *4.3* *7.7*	107 Iso *21.5*	d = 4.39 nm (100)	0.48 (100)	720 (90)
Si$_4$B5	Cr 67 $\mathrm{SmCP_{FE}}^{[*]}$ *13.2*	107 Iso *22.5*	d = 4.73 nm (90)	0.46, 0.60 (90)	810 (100)
Si$_{4t}$B5[d]	Cr 76 SmC$_s$P$_F$ 91 Col$_{ob}$P$_A$ *17.4* *2.3*	107 Iso *17.9*	a = 2.22 nm, b = 4.64 nm, γ = 95° (99); d = 4.54 nm (80)	0.48 (80)	670 (100), 700 (80)
Si$_1$B6[e]	Cr$_1$ 99 Cr$_2$ 108 $\mathrm{SmCP_{FE}}^{[*]}$ *2.9* *15.3*	165 Iso *26.0*	d = 4.13 nm (140), 4.12 nm (90)	0.47 (140), 0.46 (115), 0.44 (30)	740 (130)
Si$_2$B6[e]	Cr 85 $\mathrm{SmCP_{FE}}^{[*]}$ *9.1*	165 Iso *27.2*	d = 4.49 nm (130)	0.46, 0.58 (130)	780 (130)
Si$_3$B6[e]	Cr$_1$ 57 Cr$_2$ 74 Cr$_3$ 88 $\mathrm{SmCP_{FE}}^{[*]}$ *6.7* *11* *4.7*	162 Iso *29.5*	d = 4.76 nm (150), 4.80 nm (70)	0.46, 0.57 (120)	740 (130)
Si$_{3i}$B6[e]	Cr 94 $\mathrm{SmCP_{FE}}^{[*]}$ *16.8*	165 Iso *29.6*	d = 4.71 nm (155), 4.77 nm (75)	nd	820 (120)
Si$_{4t}$B6[e]	Cr 65 $\mathrm{SmCP_{FE}}^{[*]}$ *8.9*	171 Iso *29.3*	d = 5.00 nm (160), 5.06 nm (130), 4.95 nm (60), 4.90 nm (25)	0.48 (130); 0.44, 0.52 (60)	730 (120)
Si$_2$B$_2$6	Cr 80 $\mathrm{SmCP_{FE}}^{[*]}$ *7.0*	167 Iso *25.0*	d = 4.62 nm (120)	0.46, 0.58 (120)	720 (130)
Si$_2$B$_3$6	Cr 86 $\mathrm{SmCP_{FE}}^{[*/\circ]}$ *21.0*	167 Iso *24.4*	d = 4.55 nm (130)	0.46, 0.58 (110)	710 (130)

[a] Phase-transition temperatures and enthalpies determined by DSC at 10 K/min during first heating scans from 20 °C to 200 °C for all compounds (during consecutive second heating scans from −10 to 200 °C for **Si$_3$B5** and **Si$_{3i}$B5**); however, DSC performed for **Si$_x$B6** after the isotropic melt was stored in vials at room temperature for two years; mesophases assigned by the analysis of DSCs and 2D XRD data, together with electro-optical investigations; lattice parameters and ODSs from 2D XRD data. Abbreviations: SmC$_s$P$_F$ = synclinic FE switching polar smectic phase; $\mathrm{SmCP_{FE}}^{[*]}$ = tilted smectic phase with dark conglomerate (DC) texture, where single-peak FE switching is observed ($^{[*]}$ denotes the existence of optically active domains, although the molecules themselves are achiral); $\mathrm{SmCP_{FE}}^{[*/\circ]}$ = tilted smectic phase where the dark conglomerate phase coexists with a birefringent grainy texture and single-peak FE switching is observed ($^{[*/\circ]}$ denotes the coexistence of optically active and birefringent domains); and nd = no data. [b] Numerical values given in roman font are phase-transition temperatures, expressed in units of degrees Celsius. Values given in italic font represent the phase enthalpy (ΔH), expressed in units of kJ/mol. [c] Values given in parentheses are temperature, expressed in units of degrees Celsius. [d] See ref 19. [e] Upon cooling, a transition to a glassy $\mathrm{SmCP_{FE}}^{[*]}$ state (g$\mathrm{SmCP_{FE}}^{[*]}$) occurs at 50−80 °C (see Figures S6 and S7 in the Supporting Information).

2. Mesomorphic Properties. *2.1. LC Phases of Compounds* **Si$_x$B5**: Transition from Ferroelectric Switching DC Phases to Antiferroelectric Switching Columnar Phases. The phase-transition temperatures, X-ray data, and spontaneous polarizations for all compounds are summarized in Table 1. Compounds **Si$_x$B5** exhibit optically isotropic dark conglomerate-type tilted and polar smectic phases with chiral textures ($\mathrm{SmCP_{FE}}^{[*]}$)[29] identified under slightly uncrossed polarizers (see an example in Figures 2a and 2b), except for compound **Si$_{4t}$B5**, which possesses two birefringent LC phases: a columnar phase (Col$_{ob}$P$_A$) and a SmC$_s$P$_F$ phase. Compound **Si$_1$B5** with only one Si atom and compound **Si$_2$B$_3$6** with two Si atoms and a longer aromatic core show the coexistence of dark conglomerate textures and birefringent grainy textures ($\mathrm{SmCP_{FE}}^{[*/\circ]}$). This indicates that the ratio of the size of the carbosilane unit, with respect to the length of the aromatic core, determines if a birefringent or DC-type smectic phase is observed. All mesophases are enantiotropic (thermodynamically stable) and the clearing points,

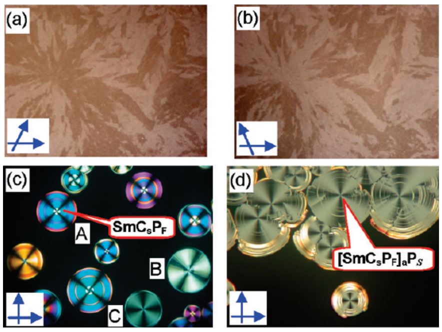

Figure 2. Textures for compound **Si_3B5** in dark conglomerate phases ($SmCP_{FE}^{[*]}$) and **$Si_{3i}B5$** under an electric field in a ITO-coated 6 μm cell: (a, b) chiral domains observed at 95 °C between slightly uncrossed polarizers (±5°); (c) circular colorful SmC_sP_F domains formed from the isotropic liquid (dark area) at 103 °C upon the application of a square wave (SW) voltage (±30 V, 0.5 Hz) during cooling; (d) circular gray $[SmC_sP_F]_aP_S$[23] domains formed from the initially developed SmC_sP_F domains at 100 °C upon the application of a SW voltage (±40 V, 200 Hz). The angles of extinction brushes with respect to crossed polarizers in panel (c) are 40° for domain A, 29° for domain B, and 3° for domain C, respectively. SmC_sP_F domains are observed as two homogeneously chiral states, whereas $[SmC_sP_F]_aP_S$[23] domains are observed as a racemic state.

i.e., the transition temperatures from the LC phases to the isotropic liquid, slightly decrease as the number of Si atoms in the linear carbosilane units increases from one to four. Nevertheless, because of the decrease of the melting temperatures in the series of compounds **Si_xB5**, the LC temperature range increases significantly as the number of Si atoms in the linear carbosilane units increases from one to three, and appears to reach a maximum when the number of Si atoms is three. In comparison with their siloxane analogues,[17] compounds **Si_xB5** (x = 2, 3, and 3i) show the same $SmCP_{FE}^{[*]}$ phase temperature range, but their clearing points are 3−9 °C lower, which might be due to the reduced dipolar interactions, resulting from the reduced polarity of the Si−C bonds, compared to the Si−O bonds. Also, the layer spacings are almost identical for both series, i.e., the structural model proposed for the LC phases of the siloxanes[11] should also be applicable for the carbosilanes.

Upon the application of a sufficiently strong external electric field, the layer distortion in these DC phases can be removed and the field-induced birefringent smectic phases behave as FE switching smectic phases. All compounds **Si_xB5** show a sharp single current peak during the half period of an applied TW voltage at both high (200 Hz) and low (0.1 Hz) frequencies in their smectic phases (see Figures 3d and 3e, as well as Figure S4 in the Supporting Information), which suggests a FE switching process, and, therefore, the DC phases were assigned as $SmCP_{FE}^{[*]}$ (for details, see section 3.1). As shown in Table 1, the measured spontaneous polarizations in both series fall well within the range of 700−850 nC/cm^2. Under a low-frequency TW field, high-birefringence circular domains with dark extinction brushes inclined to the directions of polarizer and analyzer were observed (Figure 3a). In these synclinic domains (SmC_sP_F), a rotation of the dark extinction crosses occurs after field reversal (see Figures 3a−c), confirming bistable (i.e., FE) switching via rotation on a cone.

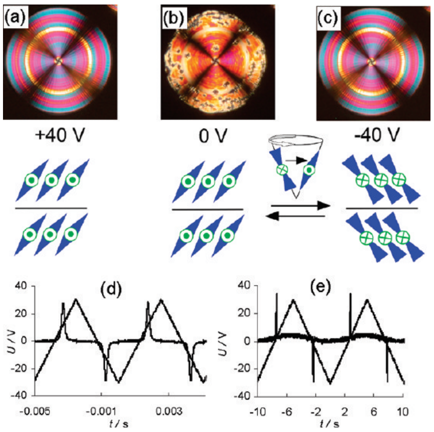

Figure 3. (a−c) Optical micrographs of a chiral SmC_sP_F circular domain and associated molecular orientation at the bottom and (d and e) switching current curves at 90 °C for compound **$Si_{3i}B5$** in a 6-μm ITO cell ((d) ±30 V_{pp}, 200 Hz; (e) ±30 V_{pp}, 0.1 Hz). The circular domain was obtained by cooling from the isotropic liquid (dark area) under a low-frequency SW voltage (±40 V, 1 Hz). The models show bistable FE switching on a cone between the two oppositely tilted arrangements of a SmC_sP_F state. The slight decrease of birefringence at 0 V might be due to a deformation leading to a local transition of the surface-stabilized FE state to the DC structure.

The incorporation of a bulky tertiary Si_{4t} unit in compound **$Si_{4t}B5$** leads to a transition from dark conglomerate-type smectic phases ($SmCP_{FE}^{[*]}$) to a columnar phase ($Col_{ob}P_A$), probably because of strong layer distortion that results from the bulky tertiary Si_{4t} unit.[19] This columnar phase is subsequently transformed to a birefringent low-temperature smectic phase (SmC_sP_F), perhaps due to the decrease of layer distortion at low temperature. In this case, the synclinic organization of the molecules was proven by X-ray evidence. The fact that this SmC_sP_F phase shows switching and electro-optical properties very similar to those of the other carbosilane analogues **Si_xBm** supports a synclinic tilted organization of the molecules in the DC phases of compounds **Si_xBm**.

2.2. LC Phases of Compounds **Si_xB6**: Glassy Dark Conglomerate (DC) Phases. Similar to compounds **Si_xB5**, compounds **Si_xB6** also exhibit DC smectic phases with chiral textures (see Figure S5 in the Supporting Information). However, the transition temperatures from the $SmCP_{FE}^{[*]}$ phases to the isotropic liquid significantly increase from ~110 °C for compounds **Si_xB5** to ~165 °C for compounds **Si_xB6**, indicating that elongation of the core by one phenyl ring significantly stabilizes the $SmCP_{FE}^{[*]}$ phases and also leads to wider $SmCP_{FE}^{[*]}$ phase ranges.

Moreover, in contrast to compounds **Si_xB5**, which crystallize within a temperature range of 64−110 °C, the DC phases of compounds **Si_xB6** are retained down to room temperature and no crystallization was observed during storage at room temperature from several days up to months. In the DSC cooling scans, only one exothermic peak, which was attributed to a transition from the isotropic liquid to the DC phases ($SmCP_{FE}^{[*]}$), was observed besides a broad glass-transition step between 50 °C and 80 °C (see Figures S6 and S7 in the Supporting Information). These observations indicate that the DC phases of compounds **Si$_x$B6** are supercooled to the glassy state (gSmCP$_{FE}$$^{[*]}$). This is consistent with XRD investigations on compound **Si$_1$B6**. During cooling from 140 °C to 30 °C, we did not observe any significant change in the diffraction patterns (see Figure S8 in the Supporting Information), except that the layer spacing slightly decreases from 41.3 Å (140 °C) to 40.3 Å (30 °C), indicating that the smectic phase is retained in the glassy state (see Figures S8 and S9 in the Supporting Information). Optical investigations indicate that the chiral textures remain when cells were cooled to room temperature and stored at room temperature for weeks. Since the supercooled glassy state is metastable, crystallization can slowly occur during storage and the speed of crystallization depends on the temperature and the size of the carbosilane termini. The smaller the carbosilane units, the quicker crystallization proceeds (several days to several months). For most compounds, upon heating, the glassy state directly melts to the fluid DC phase. Partial crystallization is observed during softening of the glass only for compounds **Si$_1$B6** and **Si$_{3i}$B6**, indicated by an exothermic peak shortly above the glassy state at ≥80 °C (see Figure S6a in the Supporting Information).

Similar to compounds **Si$_x$B5**, dark conglomerate (DC) phases in compounds **Si$_x$B6** also show FE switching (see Figure S10 in the Supporting Information) upon the application of a TW voltage during both heating and cooling, and the measured spontaneous polarizations are in the same range. The FE switching gradually stops at ~50 °C during cooling, confirming a glassy solidification. The field-induced birefringent texture is retained in the glassy state. Hence, crystallizaton from the field-induced flat layer structures is obviously inhibited in the supercooled glassy state.

The threshold voltage at which FE switching is induced for the SmCP$_{FE}$$^{[*]}$ phases with chiral domains (as obtained either by cooling from the isotropic liquid or by heating from the gSmCP$_{FE}$$^{[*]}$ state) varies between ~3 V/μm for **Si$_2$B6** (at 80 °C) and ~17 V/μm for **Si$_2$B$_2$6** (at 90 °C). However, for the same compounds with flat layers, once induced under an electric field and then frozen in the glassy state,[30] the threshold voltage required for polar switching (above the glass-transition temperature) is much lower (0.3−1.0 V/μm at 80 °C).[31] This supports the idea that DC phases represent lamellar phases that have spongelike deformed layers[7] (see Figure 5c) and indicates that the removal of layer deformation to generate flat layers requires much more energy than molecular switching in these flat layers.

2.3. Influence of Position and Number of Biphenyl Units on the Mesomorphic Properties. To examine the effect of the position and number of biphenyl units on DC phases, we synthesized compound **Si$_2$B$_2$6**, which is a positional isomer of **Si$_2$B6** that contains a terminal biphenyl unit, and compound **Si$_2$B$_3$6**, which contains one central and one terminal biphenyl unit. As shown in Table 1, both compounds **Si$_2$B6** and **Si$_2$B$_2$6**, incorporating only one biphenyl unit, exhibit ground-state DC phases that exhibit field-induced FE switching behavior, while compound **Si$_2$B$_3$6**, incorporating two biphenyls, exhibits the coexistence of birefringent and chiral textures. Moreover, the threshold voltage required for FE switching (at 90 °C, 10 Hz) increases from **Si$_2$B$_3$6** (~1 V/μm) via **Si$_2$B6** (~3 V/μm) to **Si$_2$B$_2$6** (~17 V/μm), suggesting that **Si$_2$B$_2$6** has the most strongly deformed layers that require the highest energy to remove layer deformation. Thus, we can come to the conclusion that the increase of the number of biphenyl units in the core, e.g., in compound **Si$_2$B$_3$6**, favors flat layer organization (i.e., birefringent textures), thereby inhibiting layer deformation. Replacement of the biphenyl central core of **Si$_2$B$_3$6** by a resorcinol central core in **Si$_2$B$_2$6** leads to a DC phase requiring especially high voltage to remove layer deformation, indicating especially strongly deformed layers. Comparing **Si$_2$B6** with **Si$_2$B$_2$6** also indicates that, for molecules with the same core length, a bent resorcinol central core favors layer deformation more strongly than a biphenyl central core.

2.4. X-ray Investigation of Smectic Phases: Nanosegregation and Tilt. X-ray investigations indicate layer structures without in-plane order for all compounds except for the high-temperature phase of **Si$_{4t}$B5**, which is a columnar phase (Col$_{ob}$P$_A$, for two-dimensional (2D) unit-cell parameters, see Table 1; for details, see ref 19). The layer thickness is always much smaller than the calculated molecular length, which is consistent with a highly tilted organization of the molecules within the layers. The tilt angles θ calculated using $\cos\theta = d/L$ (where d is the layer spacing and L is the calculated molecular length via molecular modeling[32]) are in the range of 45°−51° (see details in Table S1, given in the Supporting Information). Since most compounds exhibit ground-state DC phases that prevent us from achieving any alignment for 2D XRD analysis, we could not obtain the tilt angles directly from such experiments. However, for compound **Si$_{4t}$B5**, good alignment was obtained in the high-temperature columnar phase, which was retained in its low-temperature smectic phase. Thus, a tilt angle of 46° could be derived from the distribution of the wide-angle outer diffuse scattering (ODS) (see ref 19 for details), which is in good agreement with the calculated tilt angle and also with those obtained for siloxane analogues.[11]

---

(30) Circular SmC$_s$P$_F$ domains with extinction brushes inclined to crossed polarizers are initially generated for compounds Si$_x$*B6* upon cooling the isotropic liquid under a low-frequency electric field above the threshold voltages. They quickly transform to circular [SmC$_s$P$_F$]$_a$P$_S$ domains with extinction brushes parallel or perpendicular to crossed polarizers when a high-frequency electric field is applied. [SmC$_s$P$_F$]$_a$P$_S$ textures are retained in the glassy state when cells are cooled to room temperature and stored overnight at room temperature.

(31) When cells with supercooled [SmC$_s$P$_F$]$_a$P$_S$ textures were stored overnight at room temperature and reheated to 80 °C, the threshold voltages at which FE switching occurs are 0.3−1.0 V/μm, which are much less than those that induce FE switching from the supercooled glassy state of DC phases.

(32) The molecular geometry was optimized by MOPAC calculations using the AM1 Hamiltonian. The molecular lengths are equal to the sum of the lengths of the molecular long axis from molecular modelling and twice the van der Waals radius (0.12 nm) of the H atom.

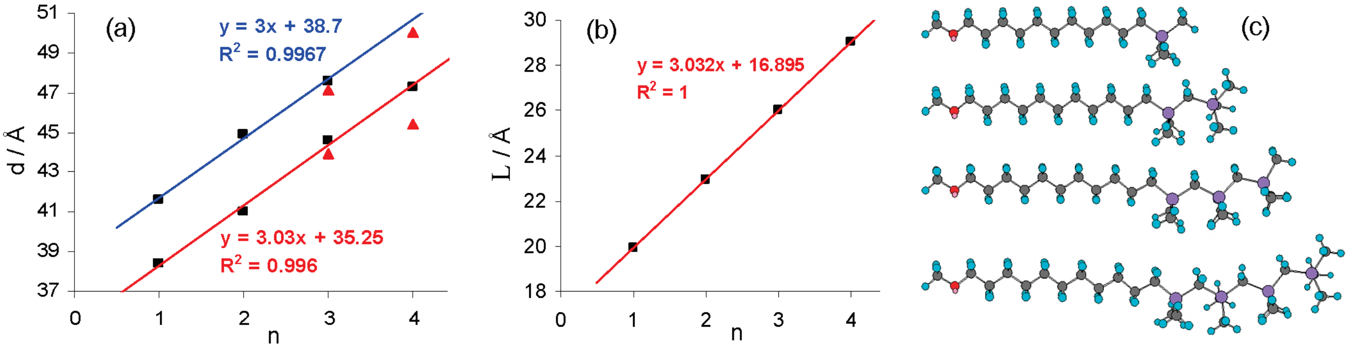

Figure 4. Plots of (a) layer spacings (d), as a function of the number of CH_2SiMe_2 segments in both compounds **Si$_x$B5** (red line) and **Si$_x$B6** (blue line) with linear carbosilane termini (denoted by solid black squares) and branched (denoted by solid red triangles) carbosilane termini, and of (b) molecular lengths (L) as a function of the number of CH_2SiMe_2 segments in compounds $MeO(CH_2)_{10}(CH_2SiMe_2)_nCH_3$ (n = 1, 2, 3, and 4), and (c) molecular conformation (purple (Si), gray (C), red (O), and cyan (H)) of compounds $MeO(CH_2)_{10}(CH_2SiMe_2)_nCH_3$ (n = 1, 2, 3, and 4) optimized by the employment of MOPAC calculations using the AM1 Hamiltonian. The treadlines in panels (a) and (b) were drawn based on data points obtained from compounds with linear carbosilane termini (denoted by solid black squares, ■), and the slopes for all lines are ~0.3 nm. Well-stretched conformations in panel (c) show that carbosilane units are almost collinear with carbon chains.

Detailed studies on ODSs show a very asymmetric profile of the theta-scans in which two maxima can be separated in case of compounds **Si$_x$B5** with carbosilanes containing at least three Si atoms and compounds **Si$_x$B6** with at least two Si atoms (Figure S11). One maximum at ~0.47 nm is related to the average distance between the bent cores and between the fluid alkyl chains along the layer, and the other maximum at ~0.58 nm is assigned to the average distance between the carbosilane units. This gives evidence of microsegregation in the smectic phases of those compounds with at least two Si atoms. It should be pointed out that this is the first X-ray evidence confirming nanosegregation of carbosilane units in LC systems.[33]

The layer spacing increases as the size of carbosilane units increases in both series of compounds **Si$_x$B5** and **Si$_x$B6** (see Table 1 and Figure 4a). The growth of the layer spacing with the number of $-CH_2SiMe_2-$ segments is almost linear, with an increment of ~0.3 nm per segment in compounds with linear carbosilane termini. To obtain the effective length of the silyl-terminated chains, depending on the number of $-CH_2SiMe_2-$ units, we determined the molecular length (L)[32] of compounds $MeO(CH_2)_{10}(CH_2SiMe_2)_nCH_3$ (n = 1, 2, 3, and 4), which mimic the flexible carbosilane tails in both **Si$_x$B5** and **Si$_x$B6**, by molecular modeling. The molecular geometry (Figure 4c) was optimized by the employment of MOPAC calculations using the AM1 Hamiltonian. The plot of the molecular length versus the number of CH_2SiMe_2 segments (Figure 4b) shows the same increment of ~0.3 nm per CH_2SiMe_2 segment, similar to that of the layer spacing in both **Si$_x$B5** and **Si$_x$B6** within experimental error. In compounds **Si$_x$B5** and **Si$_x$B6** (x = 3i, 4t) with branched carbosilane termini, layer spacings are always smaller than those in compounds that include linear carbosilane units with the same number of Si atoms (see data points denoted as solid red triangles in Figure 4a), but are larger than expected for the length provided by the linear $-SiCH_2SiMe_3$ or $-Si(CH_2)_2SiMe_3$ segments, respectively, indicating that the volume of the silyl groups also is important for layer spacing.

Since microsegregation of the carbosilane moieties was observed by XRD, we suggest a triple-layer model to describe the organization of these bent-core molecules. The molecules are likely to adopt an antiparallel packing (Figure 5a) instead of a parallel packing (Figure 5b). In this antiparallel packing model, the orientation of linear carbosilane units can be described by the equation

$$(2 - x)\cos\varphi = 1$$

where x is the ratio between the interdigitated part of a carbosilane segment and its total length, and φ is the angle between layer normal and orientation of linear carbosilane segments (see detailed discussion in Figure S12 in the Supporting Information). Full interdigitation of the silyl units (x = 1, φ = 0°) is most likely and compatible with the observed increase of the layer spacing by ~0.3 nm per $-CH_2SiMe_2-$ segment. The larger area required by the interdigitated carbosilane segments at the interlayer interfaces can be compensated by folding of the alkyl chains (spacers and terminal chains) and by a tilted organization of the aromatics. This chain folding increases the number of chain segments that are strongly tilted or even parallel to the layers, and this could give rise to the observed difference between optical tilt (40°) and the calculated tilt from layer spacings (45°−51°). This intercalated organization of the carbosilane segments would not require any tilt of the carbosilanes. Although this structure, combining highly tilted aromatics and a preferred organization of the carbosilane units on average parallel to the layer normal, appears most likely, we cannot completely rule out the possibility that there is some tilt of the carbosilanes associated with a slightly

---

(33) In all previous cases, carbosilanes had two or three CH_2 groups between the Si atoms. For this reason, these carbosilanes behave similar to branched alkyl chains and only the mean distance between the CH_2 and CH_3 groups, overlapping with the mean distances between the alkyl chains and aromatic segments (at 0.45 nm), were recorded in the XRD patterns.[18,20,21] In the case of the carbosilanes reported herein, the dense packing of the CH_3 groups provides a larger distance between these units with a mean distance of 0.58 nm.

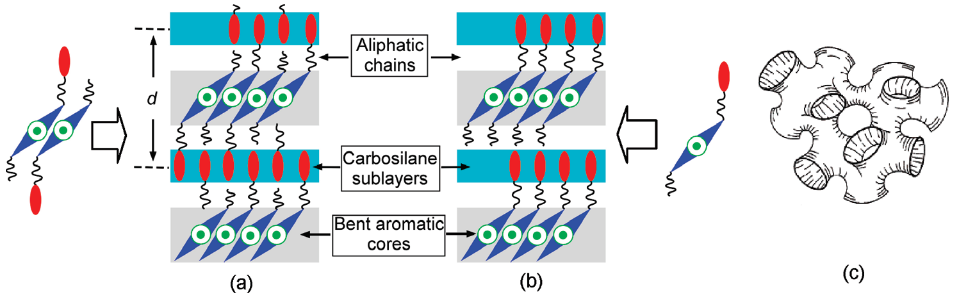

Figure 5. Models of the organization of bent-core molecules **Si$_x$Bm** with carbosilane units in a triple-layer structure with (a) antiparallel dimeric packing with full interdigitation of carbosilane units, and (b) parallel single molecular packing without interdigitation of carbosilane units. Panel (c) shows a model of a sponge phase (from ref 16b). Cyan regions represent carbosilane sublayers. Carbosilane units are drawn in red only for differentiation.

reduced degree of intercalation of these units. Partly intercalated or nonintercalated organizations of the carbosilane units should be more important for compounds with branched carbosilane units **Si$_{3i}$Bm** and **Si$_{4t}$Bm**, respectively.

3. Electro-optical Investigations of the Smectic Phases. *3.1. Transition from DC Phases to Field-Induced* SmCP$_F$ *Phases and Irreversible Structural Transformation from* SmC$_s$P$_F$ *to* [SmC$_s$P$_F$]$_a$P$_S$. A typical feature of the smectic phases of compounds **Si$_x$B5** (x = 1, 2, 3, 4, and 3i) is the formation of circular domains upon cooling their isotropic liquid under a low-frequency square wave (SW) voltage. The high-birefringence domains (see Figure 2c) formed in this way have the extinction crosses inclined to the direction of the polarizer and analyzer, indicating a synclinic SmC$_s$P$_F$ structure of the field-induced smectic phases. Upon the application of a high-frequency SW voltage these high-birefringence domains rapidly transform to low-birefringence domains with extinction crosses coinciding with the directions of polarizer and analyzer (Figure 2d), interpreted as a [SmC$_s$P$_F$]$_a$P$_S$ phase composed of SmC$_s$P$_F$ layer stacks, separated by anticlinic defect layers.[23]

In the most colorful (high-birefringence) circular SmC$_s$P$_F$ domains, shown in Figure 2c, the extinction brushes are inclined to the directions of the polarizer and analyzer by 40° (domains A), while there are two domains that have smaller angles (29° for domain B and 3° for domain C) between extinction brushes and crossed polarizers and low birefringence as well. This suggests a nonequal distribution of oppositely tilted (+)- and (−)-SmC$_s$P$_F$ stacks in the domains with smaller angles. This nonhomogenously chiral structure is assigned as (Ξ)-[SmC$_s$P$_F$]$_a$P$_S$ (see Figure S13 in the Supporting Information for the structural organization of the bent-core molecules in synclinic circular domains), where (Ξ) indicates the configurational inhomogeneity of the system.[22,34] The angles are determined by the ratio between the homogeneously chiral SmC$_s$P$_F$ stacks. Similar observations were previously reported for siloxane compounds[22] and for a Schiff-base compound.[23b] Although it is unknown whether (+)- and (−)-SmC$_s$P$_F$ stacks are periodic or not,[35] the enantiomeric excess (ee) between them can be estimated by the ratio between the angles of extinction brushes, with respect to crossed polarizers and the maximum optical tilt angle provided by circular domains with uniform SmC$_s$P$_F$ structures. For instance, if the optical tilt angle for compound **Si$_{3i}$B5** is assumed to be 40°, the maximum angle observed in synclinic circular domains (see Figure 2c), the ee values of domains B and C are estimated to be 72.5% and 7.5%, respectively. Hence, the domains with extinction brushes coinciding with the directions of the polarizer and analyzer (see Figure 2d) are similarly assigned as [SmC$_s$P$_F$]$_a$P$_S$ (see Figure S14 in the Supporting Information for the structural organization of the bent-core molecules in anticlinic circular domains), in which (+)- and (−)-SmC$_s$P$_F$ stacks have an equal ratio (ee = 0%).

Also, the application of a low-frequency TW or SW voltage to the DC phases, above a distinct threshold voltage, leads to highly birefringent textures, indicating the formation of a synclinic tilted SmC$_s$P$_F$ structure, which transforms to a [SmC$_s$P$_F$]$_a$P$_S$ structure at higher frequency.

The speed of the transformation from synclinic (SmC$_s$P$_F$) to anticlinic circular domains ([SmC$_s$P$_F$]$_a$P$_S$) strongly depends on the frequency of the applied electric field and the size of the carbosilane units. In general, at low frequency, this transition is slow, whereas high frequency accelerates this transition. Under the same frequency, compounds with bulkier carbosilane units (e.g., branched carbosilane termini) tend to have more-stable synclinic domains. The field-induced gradual transformation from a synlinic circular domain (SmC$_s$P$_F$) to an anticlinic circular domain ([SmC$_s$P$_F$]$_a$P$_S$) is shown in Figure 6 for compound **Si$_{3i}$B5** as an example. Cooling the isotropic liquid under a low-frequency SW voltage (±40 V, 1 Hz) initially induced synclinic (chiral) circular domains (Figure 6a), the subsequent application of a high-frequency field (±40 V, 200 Hz) led to a transition to anticlinic (racemic) circular domains (Figure 6h).

It is important to note that this transformation from SmC$_s$P$_F$ to [SmC$_s$P$_F$]$_a$P$_S$ in the smectic phases of compounds **Si$_x$Bm** (with exception of **Si$_{4t}$B5**) is *irreversible*, i.e., the ([SmC$_s$P$_F$]$_a$P$_S$ structure, once formed, cannot be

---

(34) The classic SmC$_a$P$_F$ structure is in conflict with our observation that the low-birefringence circular domains can have extinction crosses slightly inclined with the directions of polarizers (Figure 2c).

(35) The nonperiodic SmC$_s$P$_F$ layer stacks would be entropically more favorable.

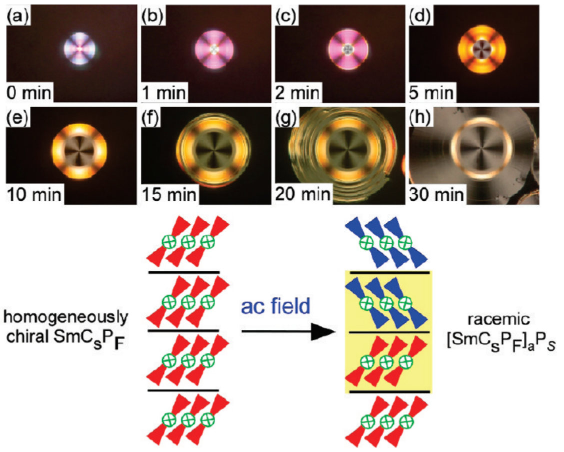

Figure 6. Field-induced transformation from a SmC$_s$P$_F$ circular domain (a) to a [SmC$_s$P$_F$]$_a$P$_S$ circular domain (h) in a 6.0-μm ITO cell for compound **Si$_{3i}$B*5***: (a−e) 103 °C, (f) 100 °C, and (g and h) 90 °C. Dark area represents the isotropic liquid. All pictures cover exactly identical areas.

transformed to the SmC$_s$P$_F$ structure, regardless of whether a low-frequency TW or SW voltage is applied. This indicates that the [SmC$_s$P$_F$]$_a$P$_S$ state is thermodynamically more stable than the uniform SmC$_s$P$_F$ states, most probably because of the increased entropy of the [SmC$_s$P$_F$]$_a$P$_S$ structure, which is composed of (irregular) layer stacks.[35] This might be surprising because, generally, among the two possible ferroelectric structures, the synclinic SmC$_s$P$_F$ structure is entropically favored, with respect to the anticlinic SmC$_a$P$_F$ structure, because of increased interlayer fluctuations in the synclinic SmC$_s$P$_F$ structure (see Figure S2b in the Supporting Information). However, for the silylated compounds, the carbosilane sublayers distort interlayer fluctuations (see Figure S2d in the Supporting Information) and, hence, the contribution to entropy becomes less important. In this case, the entropy gain achieved by mixing SmC$_s$P$_F$ layer stacks with SmC$_a$P$_F$ defect layer structures could become dominating, thereby favoring the [SmC$_s$P$_F$]$_a$P$_S$ structure. Thus, thermodynamical equilibrium is on the side of [SmC$_s$P$_F$]$_a$P$_S$, and the transformation from SmC$_s$P$_F$ to [SmC$_s$P$_F$]$_a$P$_S$ is irreversible. This is additionally supported by the fact that this transformation is greatly accelerated at high temperature, where entropy becomes more important. This transformation involves a diastereomeric structural change from homogeneously chiral SmC$_s$P$_F$ structures to racemic [SmC$_s$P$_F$]$_a$P$_S$ structures,[36,37] Because this transformation cannot be realized via only one of the two known switching mechanisms (i.e., rotation of molecules (i) on a cone or (ii) around the molecular long axis) and requires a combination of both mechanisms, it is hindered under low-frequency fields. However, it seems to become possible under a dynamic electric field with sufficiently high frequency.[38]

3.2. Irreversible Structural Transformation from SmC$_s$P$_F$ *to* [SmC$_s$P$_F$]$_a$P$_S$ *Observed via Switching Current Responses.*

Compound **Si$_{3i}$B*6*** with a branched silyl group possesses a glassy state of the DC phase at room temperature. When an 11-μm-thick ITO-coated cell filled with **Si$_{3i}$B*6*** (gSmCP$_{FE}$$^{[*]}$ state) was heated from room temperature with application of a TW voltage (±60 V$_{pp}$, 10 Hz), switching was observed at ≥80 °C, accompanied by a transition from the low-birefringence DC texture[39] to a high-birefringence grainy texture. At 115 °C, a complete transition to the high-birefringence texture (Figure 7d) was observed with a single peak (FE switching) during the half period of the applied TW voltage (Figure 7c). Hence, this birefringent texture was assigned to a SmC$_s$P$_F$ structure. When the temperature was increased to 120 °C, some high-birefringence domains changed to low-birefringence domains (Figure 7f) and a second polarization peak (Figure 7e) gradually appeared. This is interpreted as a structural transition from SmC$_s$P$_F$ to [SmC$_s$P$_F$]$_a$P$_S$, similar to the transition seen optically (Figure 6). With further increase of temperature, the initial polarization peak became smaller and the second polarization peak became larger. Finally, the high-birefringence texture is completely transformed to the low-birefringence texture (Figure 7n) at 135 °C and only the second polarization peak remained, indicating a complete transition to the [SmC$_s$P$_F$]$_a$P$_S$ structure. The same transformation was also observed for compounds **Si$_{4t}$B*6*** and **Si$_3$B*6***.[40]

In all investigated cases, the threshold voltages for FE switching in [SmC$_s$P$_F$]$_a$P$_S$ states with anticlinic interlayer interfaces are slightly higher than those in synclinic SmC$_s$P$_F$ states (1.4 vs 1 V/μm for **Si$_{3i}$B*6***, 1.5 vs 1 V/μm for **Si$_3$B*6***, and 0.7 vs 0.6 V/μm for **Si$_{4t}$B*6***),[41] suggesting that the anticlinic interfaces make switching via rotation

---

(36) Similar transformations in FE switching bent-core materials: (a) Reddy, R. A.; Dantlgraber, G.; Baumeister, U.; Tschierske, C. *Angew. Chem.* **2006**, *118*, 1962–1967. *Angew. Chem., Int. Ed.* **2006**, *45*, 1928−1933. (b) Zhang, Y.; Wand, M.; O'Callaghan, M. J.; Walker, C. M.; Thurmes, W. *Ferroelectrics* **2006**, *344*, 11.

(37) A related reversible transition was observed for AF switching bent-core mesogens where AC and TW fields stabilize the racemic SmC$_s$P$_A$ structure and DC or SW fields favor the chiral SmC$_s$P$_F$ structures, which relax to the chiral SmC$_a$P$_A$ structures upon switching off the fields: (a) Jakli, A.; Lischka, C.; Weissflog, W.; Pelzl, G.; Rauch, S.; Heppke, G. *Ferroelectrics* **2000**, *243*, 239–247. (b) Heppke, G.; Jakli, A.; Rauch, S.; Sawade, H. *Phys. Rev. E* **1999**, *60*, 5575–5579. Here, the synclinic SmC$_s$P$_F$ organization under a SW field could be entropically favored, because it enables the out-of-plane fluctuations, whereas the transformation from SmC$_s$P$_F$ to SmC$_a$P$_F$ under a TW field (10 Hz) might be due to the fact that the SmC$_a$P$_F$ (or [SmC$_s$P$_F$]$_a$P$_S$) state has sufficient time to relax to the ground-state SmC$_s$P$_A$ structure (AF switching process).

(38) This can be considered as an interesting analogy to thermodynamic and kinetic product control in chemical reactions.

(39) In Figure 6b, chiral domains were still identified by careful observation, indicating that the transformation to flat layer SmC$_s$P$_F$ structures is incomplete in this picture.

(40) Compound **Si$_1$B*6*** does not show this transformation, because of crystallization from the glassy state upon heating. For compounds **Si$_2$B*6***, **Si$_2$B$_2$*6***, and **Si$_2$B$_3$*6*** with a small carbosilane terminus, although the transformation from DC chiral textures to high-birefringence grainy textures, finally to low-birefringence textures was also observed and became much quicker when the temperature was slowly increased, only one polarization current peak was observed all the time during the whole transformation process. This may suggest that, in cases with dicarbosilane units, there is an extremely small difference for the energy barriers of FE switching in both SmC$_s$P$_F$ and [SmC$_s$P$_F$]$_a$P$_S$ structures, thereby leading to the indistinguishable superimposition of the two switching current peaks during this transformation. While in compounds with branched or large carbosilane termini, e.g., **Si$_{4t}$B*6***, **Si$_{3i}$B*6***, and **Si$_3$B*6***, the difference of the energy barriers for FE switching in both SmC$_s$P$_F$ and [SmC$_s$P$_F$]$_a$P$_S$ states is large enough to be distinguished as two separable polarization peaks.

(41) Herein, all threshold voltages denote the peak voltages of switching current curves.

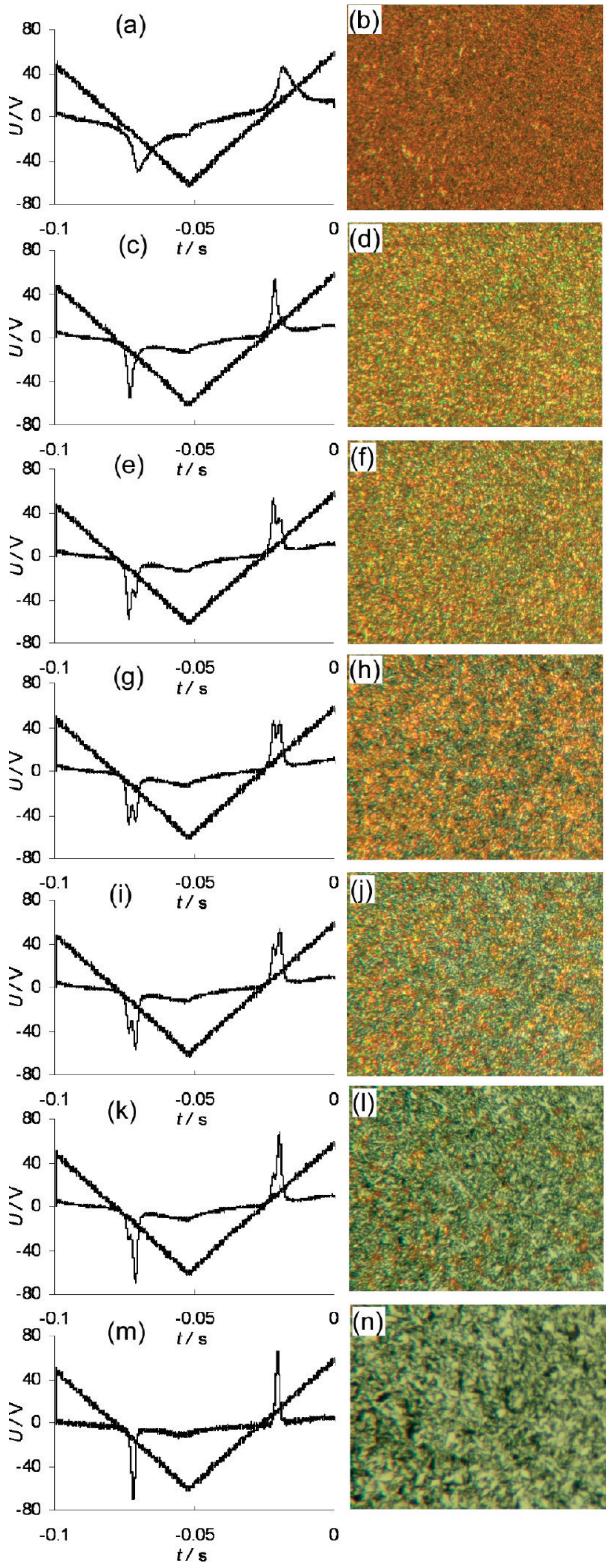

Figure 7. Sequential structural transformations of compound **Si_{3i}B*6*** from gSmCP$_{FE}$[*] via SmC$_s$P$_F$ to [SmC$_s$P$_F$]$_a$P$_S$ observed by switching current responses and texture changes with temperature and time in a 11-μm ITO-coated cell (±60 V, 10 Hz): (a, b) incomplete transformation of gSmCP$_{FE}$[*] to SmC$_s$P$_F$ at 100 °C; (c, d) only SmC$_s$P$_F$ at 115 °C; (e−l) transformation from SmC$_s$P$_F$ to [SmC$_s$P$_F$]$_a$P$_S$; (e, f) 120 °C; (g, h) 120 °C, 3 min; (i, j) 120 °C, 5 min; (k, l) 125 °C; (m, n) only [SmC$_s$P$_F$]$_a$P$_S$ at 135 °C. The brightness in pictures is not scaled, because of different exposure times.

of molecules on a cone more difficult. During this type of switching process, molecules in adjacent layers that are separated by anticlinic interfaces rotate in opposite directions, whereas those in layers separated by synclinic interfaces rotate in the same direction. This may result in a higher barrier of reorientation at the anticlinic interfaces, increasing the threshold voltage for switching in the [SmC$_s$P$_F$]$_a$P$_S$ state, incorporating anticlinic defect layers.

For compound **Si_{4t}B*6*** with the bulkiest carbosilane unit, the threshold voltages are much lower, compared to the other compounds **Si_xB*m***, which might be due to a more efficient decoupling of the layers by the silyl sublayers, because the bulky silylgroups of **Si_{4t}B*6*** are less (or not) intercalated.

4. Electro-optical Investigation of Compound Si_{4t}B*5*. *4.1. Modification of Phase Structures and Switching Behavior due to Layer Modulation.* Compound **Si_{4t}B*5*** with a short aromatic core and the bulkiest Si_{4t} terminus behaves differently from the other carbosilanes. Two LC phases were identified: Col$_{ob}$P$_A$ and SmC$_s$P$_F$.[19] Although switchable columnar phases have been reported for several other bent-core compounds,[42−44] the switching properties of the Col$_{ob}$P$_A$ phase of **Si_{4t}B*5*** are remarkable. We observed frequency-, voltage-, and temperature-dependent reversible transition from AF to FE switching[24] in this columnar phase and also a new mode of chirality flipping between oppositely tilted structures while retaining polarity.[19] This is mainly based on the temperature- and voltage-dependent complete or partial removal of layer modulation, which has a significant impact on the observed switching process.

Circular domains with extinction brushes inclined (synclinic) or coinciding with crossed polarizers (anticlinic) were induced by cooling from the isotropic liquid under a low-frequency TW or SW voltage, respectively (see

---

(42) Examples of columnar phases formed by bent-core molecules: (a) Watanabe, J.; Niori, T.; Sekine, T.; Takezoe, H. *Jpn. J. Appl. Phys.* **1998**, *37*, L139–L142. (b) Mieczkowski, J.; Gomola, K.; Koseska, J.; Pociecha, D.; Szydlowska, J.; Gorecka, E. *J. Mater. Chem.* **2003**, *13*, 2132–2137. (c) Reddy, R. A.; Sadashiva, B. K.; Raghunathan, V. A. *Chem. Mater.* **2004**, *16*, 4050–4062. (d) Pelz, K.; Weissflog, W.; Baumeister, U.; Diele, S. *Liq. Cryst.* **2003**, *30*, 1151–1158. (e) Kardas, D.; Prehm, M.; Baumeister, U.; Pociecha, D.; Reddy, R. A.; Mehl, G. H.; Tschierske, C. *J. Mater. Chem.* **2005**, *15*, 1722–1733. (f) Dierking, I.; Sawade, H.; Heppke, G. *Liq. Cryst.* **2001**, *28*, 1767–1773. (g) Nguyen, H. T.; Bedel, J. P.; Rouillon, J. C.; Marcerou, J. P.; Achard, M. F. *Pramana* **2003**, *61*, 395–404. Gorecka, E.; Vaupotic, N.; Pociecha, D.; Cepic, M.; Mieczkowski, J. *ChemPhysChem* **2005**, *6*, 1087–1093. (h) Takanishi, Y.; Takezoe, H.; Watanabe, J.; Takahashi, Y.; Lida, A. *J. Mater. Chem.* **2006**, *16*, 816–818.

(43) Examples of polar switching columnar phases of nonsilylated compounds: (a) Reddy, R. A.; Sadashiva, B. K.; Baumeister, U. *J. Mater. Chem.* **2005**, *15*, 3303–3316. (b) Umadevi, S.; Sadashiva, B. K.; Shreenivasa Murthy, H. N.; Raghunathan, V. A. *Soft Matter* **2006**, *2*, 210–214. (c) Gorecka, E.; Pociecha, D.; Mieczkowski, J.; Matraszek, J.; Guillon, D.; Donnio, B. *J. Am. Chem. Soc.* **2004**, *126*, 15946–15947. (d) Weissflog, W.; Naumann, G.; Kosata, B.; Schröder, M. W.; Eremin, A.; Diele, S.; Vakhovskaya, Z.; Kresse, H.; Friedemann, R.; Ananda Ramakrishnan, S.; Pelzl, G. *J. Mater. Chem.* **2005**, *15*, 4328–4337.

(44) Examples of polar switching columnar phases of silylated compounds: (a) Keith, C.; Reddy, R. A.; Baumeister, U.; Tschierske, C. *J. Am. Chem. Soc.* **2004**, *126*, 14312–14313. (b) Keith, C.; Dantlgraber, G.; Reddy, R. A.; Baumeister, U.; Tschierske, C. *Chem. Mater.* **2007**, *19*, 694–710. (c) See ref 22. (d) See ref 11.

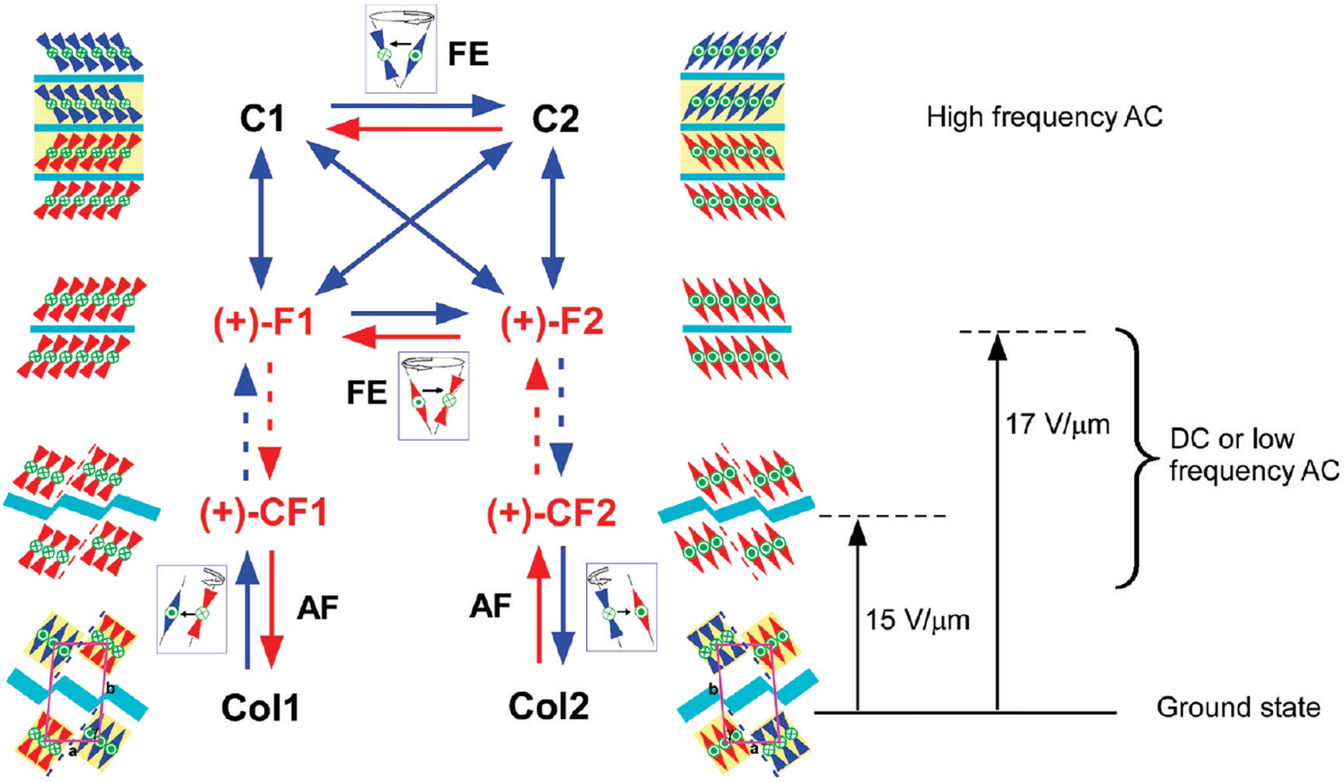

Figure 8. Transformations between different structures of compound **Si$_{4t}$B5**, as observed upon the application of an electric field. Note that 15 V/μm is the threshold field to switch the Col$_{ob}$P$_A$ (Col1 and Col2) state to the Col$_{ob}$P$_F$ (CF1 and CF2) states, and 17 V/μm is the threshold field to form the flat SmC$_s$P$_F$ (F1 and F2) layer states.[47] Color arrows represent switching via rotation of molecules either on a cone or around the molecular long axis. Color dashed arrows represent the transformation from Col$_{ob}$P$_F$ to SmC$_s$P$_F$ via removal of layer modulation. Blue double arrows show the reversible transformations between SmC$_s$P$_F$ (F1 and F2) and [SmC$_s$P$_F$]$_a$P$_S$ (C1 and C2) under a TW voltage but the detailed mechanism is unclear. Only the transformations involving the (+) states of F and CF are shown; a similar scheme can be developed for transformations involving the enantiomeric (−) states. Cyan regions represent carbosilane sublayers. AC denotes TW or SW fields.

details in Figure S15 and Table S2 in the Supporting Information). At the same frequency, to induce synclinic circular domains, a stronger electric field is required for a TW voltage than for a SW voltage (e.g., 21 vs 15 V/μm, 10 Hz).[45] At the same temperature and frequency, inducing anticlinic circular domains requires a stronger SW electric field (17 V/μm) than inducing synclinic circular domains (15 V/μm, both at 102.5 °C, 10 Hz).[46] The field-induced synclinic circular domains, obtained upon the application of a SW field above the first threshold voltage (15 V/μm), were suggested to have Col$_{ob}$P$_F$ structures with only slight layer modulation remaining from the modulated layer structure in the ground state (Col$_{ob}$P$_A$), abbreviated as CF1 and CF2 (see Figure 8). These residual modulations suppress any anticlinic organization, allowing exclusively synclinic domains. As the voltage exceeded the second threshold (17 V/μm), anticlinic circular domains with [SmC$_s$P$_F$]$_a$P$_S$ structures, abbreviated as C1 and C2, were induced, where oppositely tilted SmC$_s$P$_F$ layer stacks are separated by anticlinic and synpolar interfaces (see Figure 8).[47] It seems that above this threshold, the layer modulation is completely removed, leading to flat layer structures, similar to those observed for the field-induced polar smectic phases of the other compounds **Si$_x$B*m*** with ground-state DC phases (also see Figure 6). In these flat layers, the formation of anticlinic defect layers becomes possible, leading to the formation of the entropically favored [SmC$_s$P$_F$]$_a$P$_S$ structure. At the same temperature, but at a lower frequency (0.1 Hz) and higher voltage (33 V/μm), only synclinic circular domains were induced. This indicates that, besides a structure composed of flat layers, a dynamic field also is required to induce anticlinic defect layers, leading to the formation of [SmC$_s$P$_F$]$_a$P$_S$ structures.[48]

4.2. Frequency-, Voltage-, and Temperature-Dependent Reversible Transition from AF to FE Switching. It was found that, upon application of a TW electric field (±30 V$_{pp}$) at T = 95 C (i.e., in the temperature range of the Col$_{ob}$P$_A$ ground-state structure), the two polarization peaks seen at a low frequency (1 Hz; see Figure 9d) transform to a single

---

(45) Upon application of a TW voltage, the peak voltage is always higher than the threshold, because a certain period of time with the voltage above the threshold is required to achieve complete switching.

(46) Because the two threshold voltages are very close, synclinic and anticlinic circular domains coexist in different regions of the cell, because the field is < 17 V/μm. However, as the field becomes > 17 V/μm, only anticlinic circular domains were observed.

(47) The two slightly different polar nonmodulated states F1/F2 and the modulated states CF1/CF2 cannot be distinguished optically, but these are postulated to explain the distinct types of switching depending on the threshold voltage.

(48) The transition from [SmC$_s$P$_F$]$_a$P$_S$ to SmC$_s$P$_F$ in **Si$_{4t}$B5** upon application of a low-frequency TW field might involve an antipolar [SmC$_s$P$_F$]$_s$P$_A$ intermediate state, which could be achieved at 0 V via relaxation by rotation of molecules on a cone, which then switches to the uniform SmC$_s$P$_F$ states via rotation of the molecules around the molecular long axis upon the application of a field.

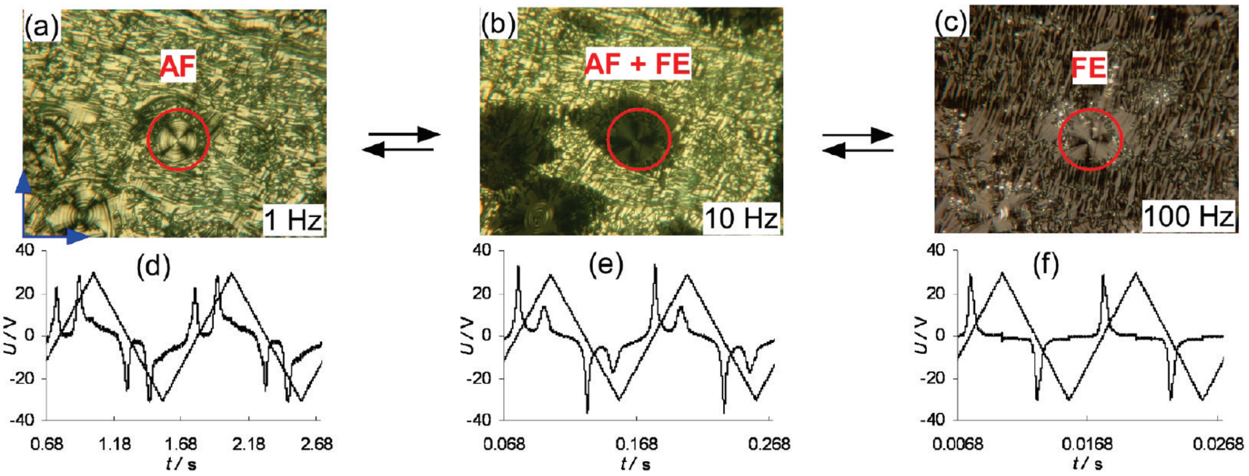

Figure 9. Frequency-dependent transformation from AF to FE switching[24] for compound **Si$_{4t}$B5** (1.2-μm ITO cell with parallel-buffed nylon alignment layers) under the applied TW voltage ($\pm$30 V$_{\mathrm{pp}}$) at 95 °C (cooling). Textures in panels (a)−(c) were developed under the applied field with different frequencies, and their switching current curves are shown in panels (d)−(f). In panel (b), AF switching occurs in high-birefringence (bright) areas, while FE switching occurs in low-birefringence (dark) areas; in panel (e), one of the two AF current peaks, attributed to relaxation from polar states to the AF state, is superimposed with the single switching current peak.

peak at a higher frequency (100 Hz; see Figure 9f). This is accompanied by a change from a high-birefringence texture with extinction crosses inclined to the directions of crossed polarizers (see Figure 9a) to low-birefringence textures with extinction crosses parallel and perpendicular to the polarizer and analyzer (see Figure 9c) (similar to the observation described previously in Figures 2d and 6h for the smectic phase of **Si$_{3i}$B5**). From the textural changes occurring upon the application of a TW electric field, it is confirmed that, under a voltage higher than the second threshold (17 V/μm), the layer modulation is completely removed, leading to field-induced flat $\mathrm{SmC_sP_F}$ layer structures (F1 and F2, see Figure 8). In these structures, switching at low frequency (1 Hz) seems to be an AF chirality switching around the long axis (two polarization current peaks, but no change of the position of the extinction crosses during switching). Under these conditions, the field-induced $\mathrm{SmC_sP_F}$ structures (F1 and F2) have sufficient time to relax to a modulated lamellar (smectic) phase composed of polar ribbons and assigned as $\mathrm{Col_{ob}P_F}$ (structures CF1 and CF2; see Figure 8) before relaxation to the apolar $\mathrm{Col_{ob}P_A}$ ground-state structure occurs. Similarly, the switching from the $\mathrm{Col_{ob}P_A}$ state to its FE states seems to be faster than removal of the layer modulation; hence, AF switching occurs between $\mathrm{Col_{ob}P_F}$ and $\mathrm{Col_{ob}P_A}$. Because of the presence of layer modulations in $\mathrm{Col_{ob}P_F}$ and $\mathrm{Col_{ob}P_A}$, this switching process can only occur by rotation around the long axis (chirality flipping; see Figure 8).[49] However, at high frequency (TW, >17 V/μm, 100 Hz), there is insufficient time for the relaxation of the field-induced flat $\mathrm{SmC_sP_F}$ structures (F1 and F2) to the modulated structures ($\mathrm{Col_{ob}P_F}$ and $\mathrm{Col_{ob}P_A}$) and a structural transition to the entropically favored $[\mathrm{SmC_sP_F}]_a\mathrm{P}_S$ structure (C1 and C2) is realized, probably via molecular reorganization, as proposed for analogues **Si$_x$B*m*** with the ground-state DC phase (see section 3). FE switching[24] occurs between the opposite polar arrangements (C1 and C2) in the field-induced (nonmodulated) $[\mathrm{SmC_sP_F}]_a\mathrm{P}_S$ state via rotation of molecules on a cone (tilt-flipping) (see Figure 8). This switching proceeds at a very low voltage (0.9 V/μm), indicating a low energy barrier between C1 and C2. The switching process itself is the same as FE switching[24] in analogues **Si$_x$B*m*** with ground-state DC phases, but the energy level of C1 and C2 should be higher than those in most other **Si$_x$B*m*** compounds, because of the ground-state apolar $\mathrm{Col_{ob}P_A}$ structure of **Si$_{4t}$B5**, in which layer modulation must be removed to obtain flat layers.[50] Hence, the switching process is modified by a field-induced transformation of the modulated layers of the virgin $\mathrm{Col_{ob}P_A}$ phase to nonmodulated flat layers ($\mathrm{SmC_sP_F}$), which are instable and, below a certain threshold voltage, relax back to the modulated smectic (i.e., ribbon) structures of the $\mathrm{Col_{ob}P_A}$ phase via the (slightly) modulated $\mathrm{Col_{ob}P_F}$ states (CF1 and CF2). Depending on temperature, there are different time scales for polar FE switching[24] and for field-induced removal of layer modulation (as well as for relaxation to a modulated structure at 0 V); therefore, a pronounced dependence on frequency and temperature is observed.

The suppression of the ribbon structure at high voltages also changes the textures, because it allows anticlinic defects, which give rise to a change of the texture from high birefringence to low birefringence and to a change of the position of the extinction crosses if a sufficiently high

---

(49) Examples for switching of chirality flipping by collective rotation around the long axis: (a) Schröder, M. W.; Diele, S.; Pelzl, G.; Weissflog, W. *ChemPhysChem* **2004**, *5*, 99–103. (b) Szydlowska, J.; Mieczkowski, J.; Matraszek, J.; Bruce, D. W.; Gorecka, E.; Pociecha, D.; Guillon, D. *Phys. Rev. E* **2003**, *67*, 031702. (c) See ref 12(m). (d) Weissflog, W.; Dunemann, U.; Schröder, M. W.; Diele, S.; Pelzl, G.; Kresse, H.; Grande, S. *J. Mater. Chem.* **2005**, *15*, 939–946. (e) Nakata, M.; Shao, R. F.; Maclennan, J.; Weissflog, W.; Clark, N. A. *Phys. Rev. Lett.* **2006**, *96*, 067802.

(50) The voltage required for removing the DC structure, depending on the molecular structure, is between 1 and 17 V/μm (see Section 2.3); in compounds **Si$_x$B5**, it is ~3 V/μm, whereas >17 V/μm is required for the removal of the 2D layer modulation in the $\mathrm{Col_{ob}P_A}$ phase of **Si$_{4t}$B5**.

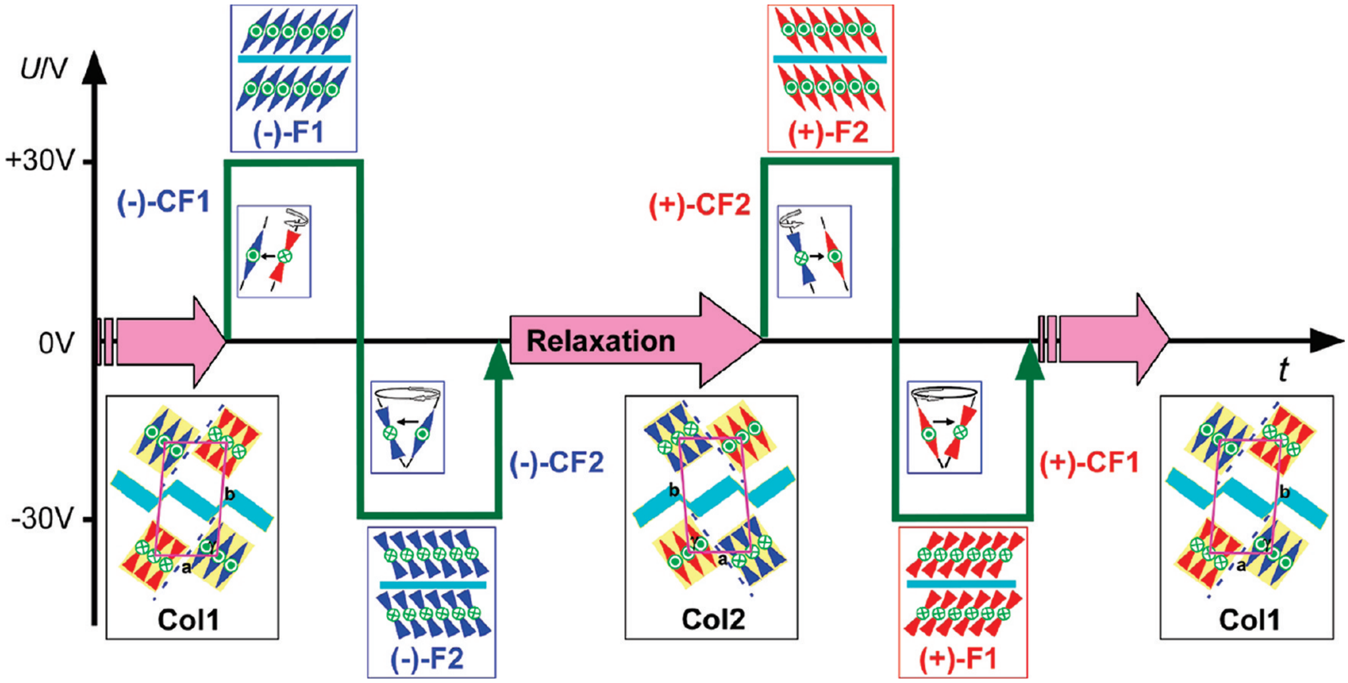

Figure 10. Application of a modified low-frequency (0.1 Hz, ±30 V) SW voltage with 0 V to allow the relaxation of polar structures to ground-state apolar structures (1.2-μm ITO cell with parallel-buffed nylon alignment layers) at 100 °C (cooling) results in the transformation from Col1 via (−)-F1, (−)-F2, Col2, (+)-F2, and (+)-F1 to Col1 via the combination of two switching mechanisms for compound $\mathbf{Si_{4t}B5}$. Col1 and Col2 represent the two oppositely tilted arrangements of the $\mathrm{Col_{ob}P_A}$ racemate at 0 V; (−)-F1 and (−)-F2 are the two oppositely tilted synclinic arrangements of the field-induced chiral flat layer (−)-$\mathrm{SmC_sP_F}$ states, and (+)-F1 and (+)-F2 are their enantiomers; (+)- and (−)-F1 (as well as (+)- and (−)-F2) have the same tilt direction but opposite chirality. CF1 and CF2 are the two field-induced $\mathrm{Col_{ob}P_F}$ structures, and similar to F1 and F2, except that they have partial layer modulation (see structures in Figure 8).

frequency is applied. Hence, the change of the switching mechanism is triggered by a field-induced structural change rather than a simple effect of changed viscosity. At intermediate frequency (±30 V_{pp}, 10 Hz) we observed an intermediate switching current curve (see Figure 9e) that contains both two-peak and single-peak switching. Under this condition, low- and high-birefringence textures (see Figure 9b) were determined to coexist in different regions of the cell, and, with increasing frequency, high-birefringence synclinic circular domains (F1 and F2) were transformed to low-birefringence anticlinic circular domains (C1 and C2).

In contrast to the *irreversible* transformation from $\mathrm{SmC_sP_F}$ to $[\mathrm{SmC_sP_F}]_a\mathrm{P}_S$, observed for other $\mathbf{Si}_x\mathbf{B}m$ with smectic DC phases, for $\mathbf{Si_{4t}B5}$, this transition is *reversible*, and by changing the frequency of a TW voltage, the structure can be changed from $[\mathrm{SmC_sP_F}]_a\mathrm{P}_S$ (C1 and C2, high frequency) to $\mathrm{SmC_sP_F}$ (F1 and F2, low frequency) and vice versa. At low frequency, there is sufficient time for the nonmodulated $\mathrm{SmC_sP_F}$ states (F1 and F2) to relax to modulated states ($\mathrm{Col_{ob}P_A}$ via $\mathrm{Col_{ob}P_F}$) and, because of the developing layer modulation, the $[\mathrm{SmC_sP_F}]_a\mathrm{P}_S$ states (C1 and C2) become disfavored, leading to removal of the anticlinic defect layers and formation of the synclinic $\mathrm{SmC_sP_F}$ states (F1 and F2, Figure 8). This indicates that the presence of a modulated ground-state structure ($\mathrm{Col_{ob}P_A}$) plays a determining role for the reversibility of this process. This is further supported by the fact that the application of a low-frequency SW voltage cannot bring $[\mathrm{SmC_sP_F}]_a\mathrm{P}_S$ back to $\mathrm{SmC_sP_F}$, since, under a SW voltage, there is no time ($t = 0$ at 0 V) for relaxation to a modulated structure, and the $[\mathrm{SmC_sP_F}]_a\mathrm{P}_S$ state is retained.[48] For the other compounds $\mathbf{Si}_x\mathbf{B}m$ with exclusively smectic phases (DC ground states), the transition from $\mathrm{SmC_sP_F}$ states to $[\mathrm{SmC_sP_F}]_a\mathrm{P}_S$ states is always *irreversible*, because there is no modulation of the layers that could destabilize anticlinic interfaces and, in this way, would disfavor the $[\mathrm{SmC_sP_F}]_a\mathrm{P}_S$ states. Hence, without layer modulation, the equilibrium is on the side of the entropically favored $[\mathrm{SmC_sP_F}]_a\mathrm{P}_S$ structures.

As shown above, the increase of the applied voltage and frequency stabilizes the single-peak polar switching,[24] and their decrease favors double-peak AF switching. In addition, the voltages and frequencies required for the induction of FE switching[24] also depend on the temperature and decrease with decreasing temperature. For example, at high temperature (100 °C), a similar transition from AF to FE switching[24] (as at 95 °C) was observed upon the application of a TW electric field, but with a higher voltage and/or higher frequencies (single peak at ±65 V_{pp}, 200 Hz, intermediate state at ±65 V_{pp}, 70 Hz, and two peaks at ±65 V_{pp}, 2 Hz, or ±30 V_{pp}, 10 Hz; see Figure S16 in the Supporting Information). At lower temperature (92 °C), two polarization peaks (Figure S17 in the Supporting Information) and high-birefringence textures were still observed upon the application of a TW electric field with a much lower frequency (0.5 Hz, ±30 V_{pp}). However, at 89 °C,[51] close to the transition to the $\mathrm{SmC_sP_F}$ phase, only one single peak (FE switching[24]) and low-birefringence textures were observed. This indicates

---

(51) DSC shows that the phase-transition temperature from $\mathrm{Col_{ob}P_A}$ to $\mathrm{SmC_sP_F}$ is 86 °C (onset) during cooling.

that, at this temperature (close to the transition to SmC$_s$P$_F$), a relatively low voltage is sufficient to remove layer modulation and the relaxation to the Col$_{ob}$P$_A$ state is slow.[52]

Thus, temperature-, frequency-, and voltage-dependent reversible transitions from AF switching by rotation of molecules around the molecular long axis (chirality switching), to FE switching[24] by rotation of molecules on a cone (tilt switching), were identified.

4.3. Chirality Flipping without Reversing Polarity. Based on the observed frequency and voltage dependence of the mode of switching, by using a special waveform combining a SW voltage with relaxation periods at 0 V, we observed unexpected field-induced transformations between the two chiral SmC$_s$P$_F$ states and their two oppositely titled arrangements—abbreviated as (+)-F1, (+)-F2, (−)-F1, and (−)-F2—and between the two oppositely tilted AF arrangements of the Col$_{ob}$P$_A$ state, abbreviated as Col1 and Col2 (see Figure 10).[19] The transformations from (−)-F2 to (+)-F2 via Col2 or from (+)-F1 to (−)-F1 via Col1 involve AF chirality switching via rotation of molecules around the long axis, while those from (−)-F1 to (−)-F2 or from (+)-F2 to (+)-F1 involve polar FE switching[24] (tilt flipping) via rotation of molecules on a cone. By combining these two transformation processes under the modified waveform, a complete cycle (Col1 to (−)-F1 to (−)-F2 to Col2 to (+)-F2 to (+)-F1 to Col1) was realized (see Figure 10) and, in this way, chirality flipping by changing tilt direction without reversing polar direction was achieved.[19] This chirality flipping requires an electric field sufficiently high[53] (above the second threshold, 17 V/μm) to induce flat layers (F1 and F2) and a relaxation period after switching off the applied SW voltage sufficiently long to allow relaxation from (−)-F2 via (−)-CF2 to Col2 and from (+)-F1 via (+)-CF1 to Col1.

The transformations between the various phase structures of compound **Si$_{4t}$B*5*** are summarized in Figure 8, which clearly connects this new mode of chirality flipping with the reversible transition from AF to FE switching.[24]

(i) Under a low-frequency SW voltage, FE switching[24] occurs between two polar structures without relaxation to another structure, since there is no time, because the voltage immediately changes its sign. If the applied SW field is higher than the first threshold, but lower than the second threshold, FE chirality switching involves a direct transition from (+)-CF1 to (−)-CF1 or from (+)-CF2 to (−)-CF2 by rotation of molecules *around the long axis* (layer modulation in CF does not allow rotation on a cone). If the applied SW field is higher than the second threshold, FE switching (tilt flipping) involves a transition from (+)-F1 to (+)-F2 or from (−)-F1 to (−)-F2 via *rotation of molecules on a cone* (flat layers prefer rotation on a cone). Modifying the frequency of the SW field does not change the fundamental switching mechanism.

(ii) Under a TW voltage, there is a dominating influence of the applied frequency. The transformation from AF to FE switching, and FE switching[24] between C1 and C2, occurs under a high-frequency voltage, because there is no sufficient time for relaxation. However, under a low-frequency field where there is sufficient time for relaxation, AF chirality switching occurs. Hence, by modifying the frequency of a TW voltage, transformations between any structure can be achieved, as shown in Figure 8 and explained in detail in section 4.2. Moreover, it is interesting to note that the transition between (−)-F1 and (+)-F2 (or (+)-F1 and (−)-F2) is the basis of the new chirality flipping process achieved by tilt flipping, as shown in Figure 10. This transition can be also realized directly by an electric field combining an abrupt change of the field direction with a slow change allowing relaxation, as provided by a SW voltage with an additional relaxation period or by a low-frequency sawtooth waveform.

Conclusion

We report the first examples of achiral polyphilic bent-core molecules (**Si$_x$B*5*** and **Si$_x$B*6***) containing a rigid aromatic core and two alkyl tails with a series of linear or branched carbosilane units at one terminus. All compounds exhibit dark conglomerate (DC) phases (SmCP$_{FE}$$^{[*]}$) with FE switching behavior upon the application of a sufficiently strong electric field with the exception of compound **Si$_{4t}$B*5***, which exhibits a columnar Col$_{ob}$P$_A$ phase (ribbon phase) at high temperature and a birefringent FE switching[24] smectic phase (SmC$_s$P$_F$) with synclinic organization at low temperature. When the number of Si atoms in the carbosilane units is at least two, microsegregation between carbosilane units and alkyl segments is identified by analyzing the profile of the outer diffuse X-ray scattering. This is the first direct observation of a microsegregation effect of carbosilane units in LC phases by X-ray methods.[33] When the carbosilane units in compounds **Si$_x$B*5*** are sufficiently large (e.g., Si$_{4t}$), a transition from a smectic phase to a columnar (ribbon) phase occurs, which is attributed to a strong layer distortion caused by this bulky group. The dark conglomerate-type phase in the series of compounds **Si$_x$B*6*** with a longer aromatic core is supercooled to the glassy state at 50−80 °C, which represents the first FE switching bent-core mesogens whose DC phases possess the glassy behavior.

X-ray studies combined with modeling indicates that the linear carbosilane units in compounds **Si$_x$B*m*** most likely adopt an orientation parallel to the layer normal with full intercalation, although the aromatic cores are highly tilted, whereas the branched carbosilane units may adopt partly intercalated or nonintercalated organizations of the carbosilane units (**Si$_{3i}$B*m*** and **Si$_{4t}$B*m***, respectively). This is of importance for understanding the effects of interlayer interfaces on molecular organization in ordered soft-matter structures.

---

(52) At this temperature, the low-birefringence circular domains have extinction crosses slightly inclined to the directions of polarizers by 5°−20°, indicating a (Ξ)-[SmC$_s$P$_F$]$_a$P$_S$ structure consisting of nonequal distribution of oppositely tilted (+)- and (−)-SmC$_s$P$_F$ stacks (see Figures 2c and S18 (in the Supporting Information)). Because the field was switched off, these domains were transformed to high-birefringence synclinic circular domains, which indicates that the field-induced structure relaxes back to the ground-state Col$_{ob}$P$_A$ phase at 0 V.

(53) Note that all threshold voltages are temperature-dependent.

Temperature- and field-dependent *irreversible* structural transitions from homogenously chiral $\mathrm{SmC_sP_F}$ to racemic $\mathrm{[SmC_sP_F]_aP_S}$ states were identified for compounds $\mathbf{Si_xB}\boldsymbol{m}$ by switching current responses and/or texture observation. Although such transitions were observed previously in the DC phases of other bent-core mesogens,[36] this is the first time that it has been shown to be associated with a change of switching current responses.

For compound $\mathbf{Si_{4t}B}\boldsymbol{5}$, an unexpected temperature-, frequency-, and voltage-dependent *reversible* transition from AF switching via rotation of the molecules around the molecular long axis to FE switching via rotation of the molecules on a cone was observed.[24] We have also identified an unprecedented field-induced supramolecular chirality flipping between oppositely tilted structures without changing polar direction in bent-core superstructures, which is distinct from the previously reported chirality switching by rotation around the molecular long axis.[49]

These investigations indicate that the combination of steric layer frustration and interlayer segregation by incorporating linear or branched carbosilane termini into bent-core mesogens can lead to new functional liquid crystalline materials with interesting characteristics and glass transitions. They also highlight the importance of the structure−property relationships in understanding and designing LC materials. The carbosilane units could be incorporated into other materials such as discotic materials and materials for field-effect transistors and photovoltaics, leading to new types of chemically stable stimuli-responsive functional materials with useful properties.

Acknowledgment. This work was supported by NSF (USA) (through Grant Nos. OII-0539835 and IIP-0646460 to Displaytech, Inc.).

Supporting Information Available: Supporting figures, tables, and descriptions, as described below: four basic structures of B2 phases (Figure S1); interlayer fluctuation (Figure S2); switching mechanisms (Figure S3); switching current responses (Figures S4, S10, S16, and S17); chiral domains of the DC phase (Figure S5); DSC curves (Figures S6 and S7); 2D X-ray patterns (Figures S8 and S9); outer diffuse scattering (Figure S11); explanation of carbosilane interdigitation in antiparallel dimeric packing (Figure S12); organization of bent-core molecules in circular domains (Figures S13 and S14); inducing circular domains from the isotropic liquid of compound $\mathbf{Si_{4t}B}\boldsymbol{5}$ (Figure S15, Table S2); textures of compound $\mathbf{Si_{4t}B}\boldsymbol{5}$ (Figure S18); calculation of tilt angles (Table S1); description of the experimental procedures and analytical data (NMR, elemental analysis) of the reported compounds. The material is available free of charge via the Internet at http://pubs.acs.org.